JOURNAL OF GEOPHYSICAL RESEARCH, VOL. 103, NO. C6, PAGES 12,899–12,918, JUNE 15, 1998

A Pacific hydrographic section at 88°W: Water-property distribution

Mizuki Tsuchiya and Lynne D. Talley

Scripps Institution of Oceanography, University of California San Diego, La Jolla

Abstract. Full-depth conductivity-temperature-depth (CTD)/hydrographic measurements with high horizontal and vertical resolution were made in February-April 1993 along a line lying at a nominal longitude of 88°W and extending from southern Chile (54°S) to Guatemala (14°N). It crossed five major deep basins (Southeast Pacific, Chile, Peru, Panama, and Guatemala basins) east of the East Pacific Rise. Vertical sections of potential temperature, salinity, potential density, oxygen, silica, phosphate, nitrate, and nitrite are presented to illustrate the structure of the entire water column. Some features of interest found in the sections are described, and an attempt is made to interpret them in terms of the isopycnal property distributions associated with the large-scale ocean circulation. These features include: various near-surface waters observed in the tropical and subtropical regions and the fronts that mark the boundaries of these waters; the possible importance of salt fingering to the downward salt transfer from the high-salinity subtropical water; a shallow thermostad (pycnostad) developed at 16°-18.5°C in the subtropical water; low-salinity surface water in the subantarctic zone west of southern Chile; large domains of extremely low oxygen in the subpycnocline layer on both sides of the equator and a secondary nitrite maximum associated with a nitrate minimum in these low-oxygen domains; high-salinity, low-oxygen, high-nutrient subpycnocline water that is carried poleward along the eastern boundary by the Peru-Chile Undercurrent; the Subantarctic Mode and Antarctic Intermediate waters; middepth isopycnal property extrema observed at the crest of the Sala y Gomez Ridge; influences of the North Pacific and the North Atlantic upon deep waters along the section; and the characteristics and sources of the bottom waters in the five deep basins along the section.

1. Introduction

A full depth hydrographic (discrete and conductivity-temperature-depth (CTD)) section with closely spaced stations was occupied across the equator in the eastern Pacific from southern Chile to Guatemala. It runs along a nominal longitude of 88°W with an additional short zonal leg connecting it to the South American coast. It constitutes the major portion of the easternmost one-time meridional hydrographic section (designated as P19) of the World Ocean Circulation Experiment (WOCE) Hydrographic Program (WHP) in the Pacific Ocean.

The fieldwork was carried out on R/V *Knorr* (Cruise 138, Leg 12) in February-April 1993. A total of 189 stations were occupied as illustrated in Figure 1. The section began at the shelf break just off the west entrance to the Strait of Magellan and extended westward along 54°S to 88°W and then northward along 88°W to 20°S. Farther north, it deflected eastward to 85°50'W to pass through the deepest portion of the Carnegie Ridge east of the Galapagos Islands. At 4°N the ship turned to the northwest parallel to the coast of Central America before turning again onshore toward the last station at the shelf break inshore of the Middle America Trench off Guatemala. The entire section was located east of the East Pacific Rise and crossed five major deep basins (Southeast Pacific, Chile, Peru, Panama, and Guatemala basins).

Station spacing was generally 56 km but reduced to 37 km between 3°and 1°S as well as between 1°and 3°N and to 19 km within 1°of the equator. Spacing was also <56 km near the Chilean and Guatemalan coasts and over Sala y Gomez Ridge (25°S) to resolve small-scale features associated with the steep topography. On each station a rosette water sampler equipped with a CTD was lowered to the bottom, and water samples were collected from a maximum of 36 levels throughout the water column.

The primary purpose of this paper is to display vertical sections of fundamental water properties in an internally consistent manner (Figures 2-9) and to describe

Paper number 97JC03415.
0148-0227/98/97JC-03415$09.00

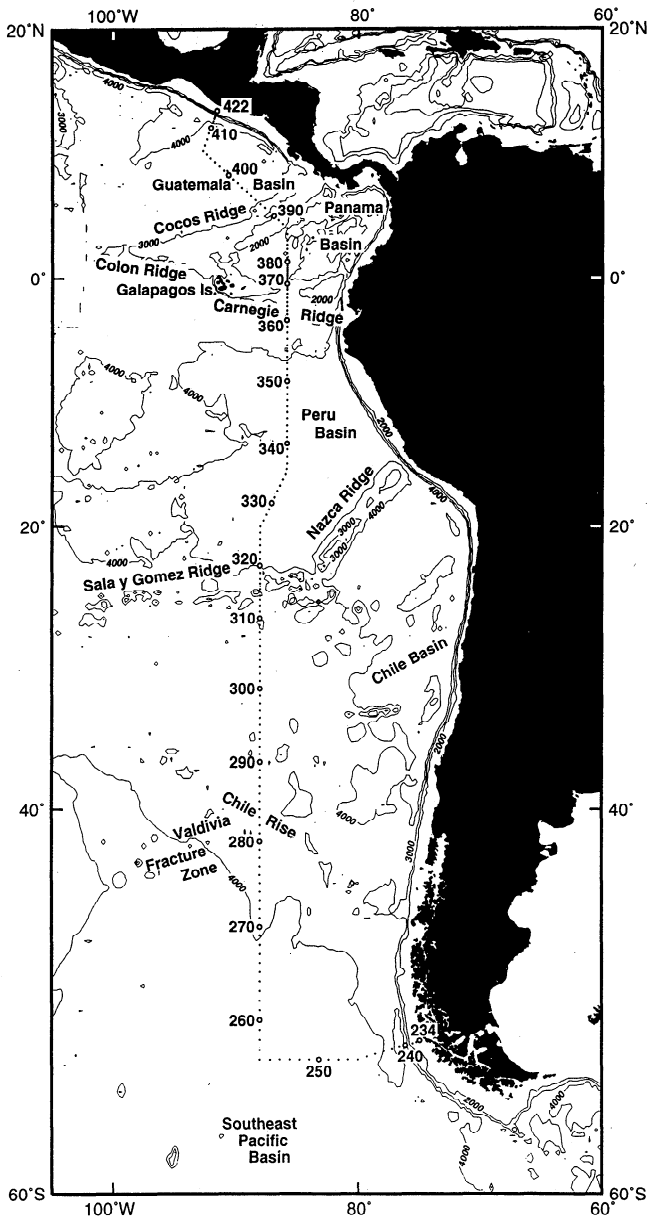

Figure 1. Positions of the stations occupied by R/V *Knorr* on Cruise 138, Leg 12 (WOCE Hydrographic Program P19C), February-April 1993 and used for the vertical sections illustrated in Figures 2-9, with the 2000-, 3000-, and 4000-m isobaths.

briefly some important features in the property distributions associated with the large-scale ocean circulation. The properties dealt with are potential temperature, salinity, and potential density (based on CTD data) and oxygen, silica, phosphate, nitrate, and nitrite (based on bottle data). All density-anomaly values (σ_θ, σ_2 etc.) in this paper are calculated according to the International Equation of State (EOS80), with the units being kg m^{-3}. Temperature values are on the International Temperature Scale of 1990 (ITS90), and salinity values are on the Practical Salinity Scale of 1978 (PSS78). The bottle salinity used to calibrate the CTD salinity is standardized with reference to P-120 standard seawater.

2. Near-Surface Waters

Warm, low-salinity surface water (θ >28°C ; S <34), separated from underlying colder, more saline water by a strongly developed thermocline and halocline, is found north of the equator. The low salinity is due in part to local rainfall and in part to westward advection of fresher water from the Panama Bight, where the surface salinity is reduced even more severely by heavy rainfall and runoff [*Wooster*, 1959]. This equatorial surface water is particularly warm and fresh just north of the equator reaching a maximum temperature of above 30°C and a minimum salinity of 31.6 near 5°N (Figure 10). It is probably associated with an anticyclonic circulation that is normally found at the surface of this region in February-March [*Puls*, 1895; *Cromwell*, 1958; *Wyrtki*, 1965; *Tsuchiya*, 1974]. On this section the warm, low-salinity surface water north of the equator is interrupted by colder, more saline water associated with an outcropping of the thermocline (halocline) at the sea surface near 8°N. This uplift of the thermocline water is also seen in the oxygen and nutrient sections (Figures 5-8) and can be identified as the Costa Rica Dome. The dome is permanent and located at the eastern end of the thermocline ridge extending zonally along the northern boundary of the North Equatorial Countercurrent, part of which turns northward to form a cyclonic circulation around the dome [*Cromwell*, 1958; *Wyrtki*, 1964a]. On this section the North Equatorial Countercurrent is clearly indicated by the northward rise of the isopycnals (Figure 4) and fall of the steric height of isobars (Figure 11) with corresponding high eastward geostrophic speeds in the upper kilometer on the southern flank of the Costa Rica Dome.

The upper portion of the thermocline rises to the sea surface also near the equator, and the colder, more saline thermocline water is exposed. Thus the surface temperature exhibits a local meridional minimum (<27°C) at the equator, and the surface salinity exhibits a local maximum (>34.6) slightly south of the equator. This feature is due to a combined effect of local equatorial upwelling and westward advection of cold Peru Current water, which has upwelled off the coast of Peru. Between the equator and the low-salinity water at 5°N are found very strong meridional gradients in temperature and salinity (Figure 10). These gradients appear to correspond to the "equatorial fronts," which extend, on the average, from 4°S at the coast of Peru toward the Galapagos Islands [*Wooster*, 1969]. The equatorial temperature minimum is accompanied by a maximum (>29°C) at 3°S, and there is a narrow band of low salinity (<34) centered at 5°S. This low-salinity water is also bounded on both sides by strong salinity gradients. It must have originated to the north of the equator and crossed it somewhere east of the present

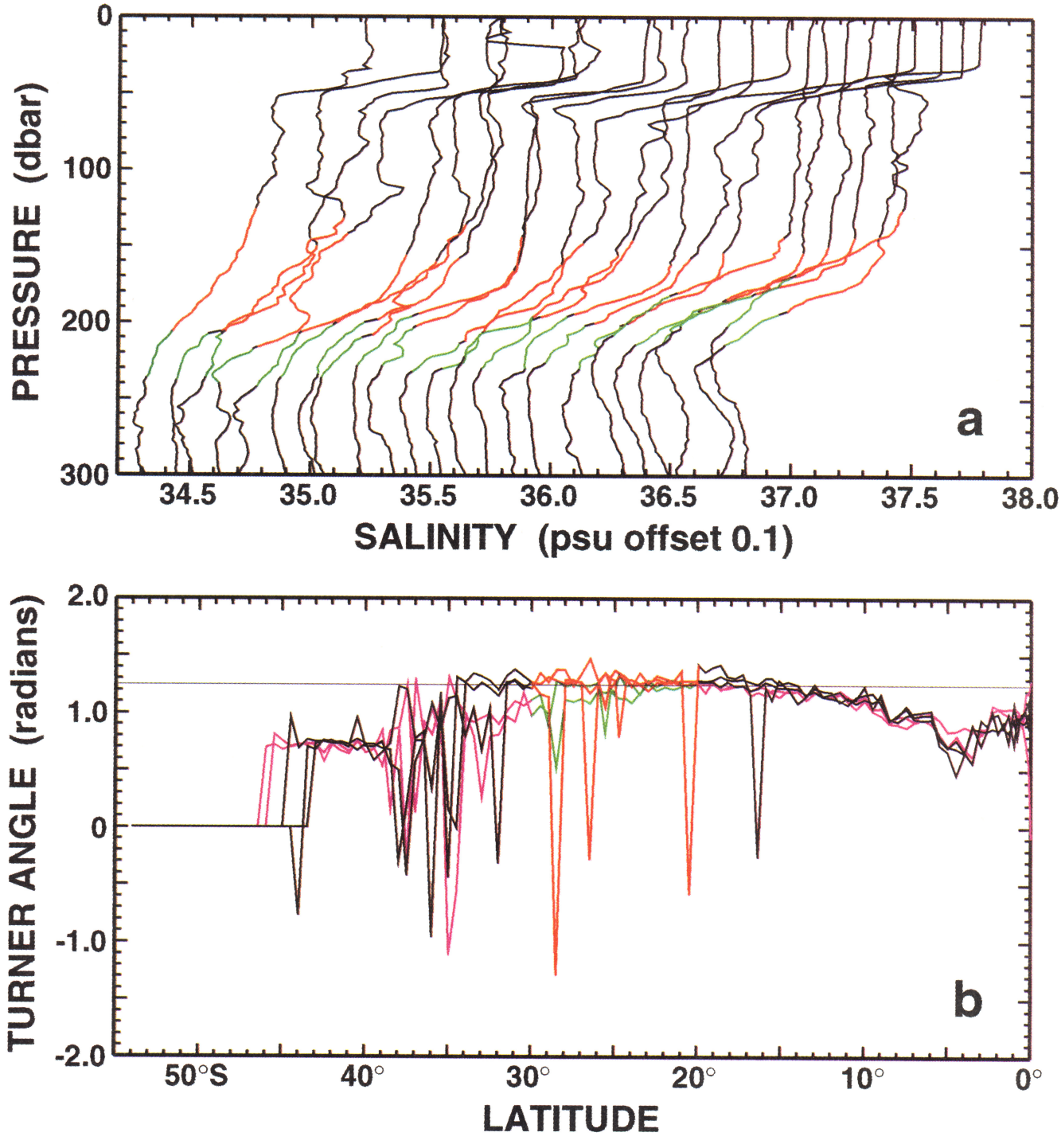

Plate 1. (a) Unsmoothed CTD salinity profiles (2-dbar resolution) along 88°W between 20°and 30°S (stations 304-326). Red portions are 25.5 to 25.75 σ_θ. Green portions are 25.75 to 25.95 σ_θ. (b) Turner angle (radian) at 25.5, 25.6 and 25.7 σ_θ (black and red) and at 25.8 and 25.9 σ_θ (purple and green) along 88°W. These densities are characteristic of the main halocline below the pycnostad. Vertical gradients of salinity and temperature are based on a least squares fit of a straight line over 10 dbar of the unsmoothed CTD data. Turner angles in excess of 1.25 suggest active salt fingering [*Ruddick*, 1983]. Highest Turner angles occur over a broad latitude range compared with other isopycnals from 25.1 to 25.9 σ_θ. Red and green curves are at stations 304-326 used in Plate 1a.

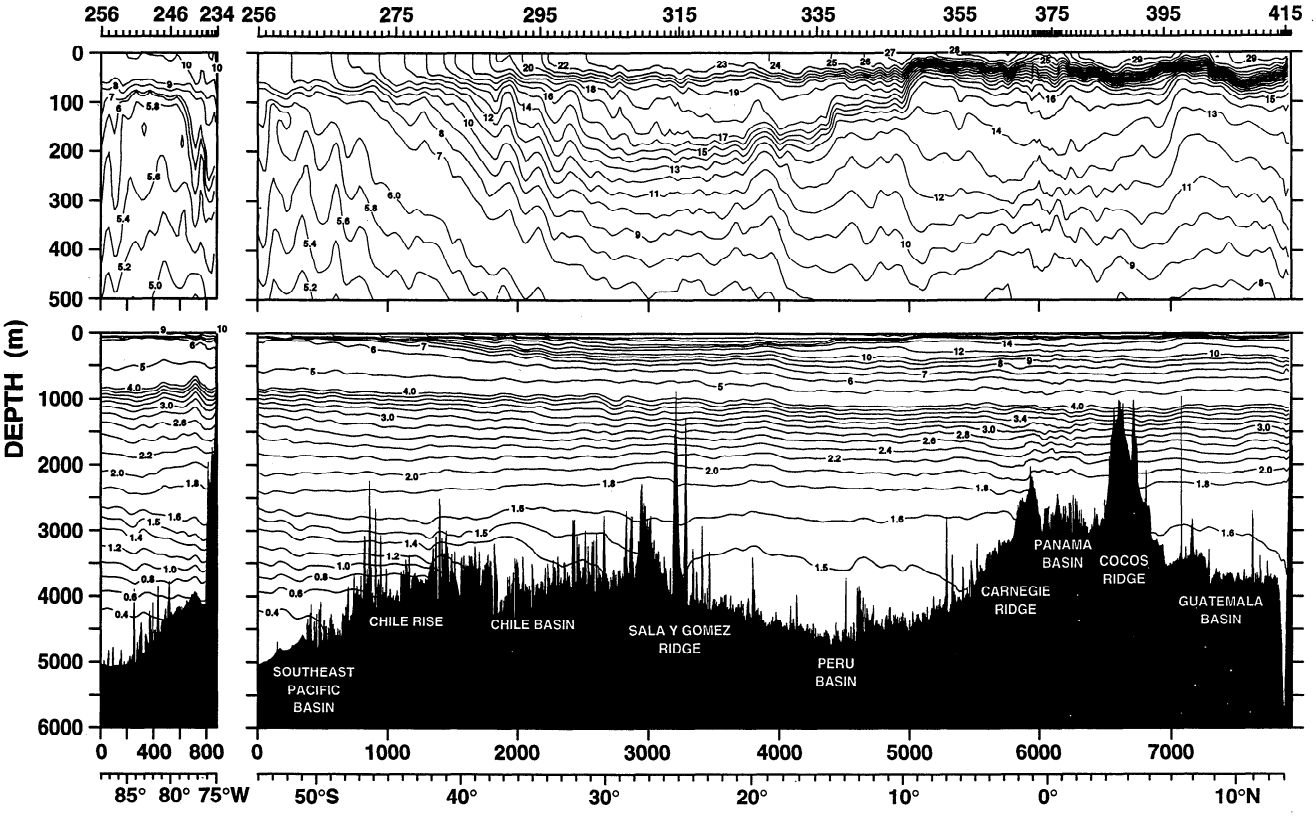

Figure 2. Potential temperature (degrees Celcius), based on conductivity-temperature-depth (CTD) data, along the section shown in Figure 1. The vertical exaggerations are: 3750 (upper panels) and 500 (lower panels). Station numbers at top of figure; latitude or longitude (degrees) and distance (kilometers) at bottom.

section. This interpretation seems plausible, because available monthly average surface temperature charts indicate that the equatorial temperature minimum is normally only weakly developed east of the Galapagos Islands during the months of February-March [e.g., *Wyrtki*, 1964b; *Robinson*, 1976].

Between about 10°and 34°S a large bowl-shaped body of highly saline, nutrient-poor water develops in the upper layer, where the permanent thermocline is depressed to a depth of 200 m. This relatively warm, highly saline water represents the eastern edge of the South Pacific subtropical water (also called tropical water), a product of excess evaporation over precipitation. The highest surface salinity (>35.9) over the entire section is found near 18°S.

The strong vertical gradients of salinity and temperature at the base of this thick layer suggest the possibility of salt finger development. The Turner angle is a convenient way of quantifying the potential for salt fingering [*Ruddick*, 1983] and is related to the more familiar density ratio. Turner angle is $\tan^{-1}(-R_\rho)$ - 45°, where R_ρ is the density ratio $\alpha\partial_z T/\beta\partial_z S$, α is the thermal expansion coefficient, and β is the haline contraction coefficient. Every combination of temperature and salinity gradients has a unique Turner angle, and the angle is also nonsingular; both are advantages in comparison with density ratio. Salt fingering is expected if warm, salty water lies above cold, fresh water and the density ratio is <2, corresponding to a Turner angle of 71.6°(1.25 rad). Maps of Turner angle have been prepared for the vertical gradients across the base of the mixed layer in the Pacific, based on the National Oceanographic Data Center's winter climatology [*Levitus et al.*, 1994; *Levitus and Boyer*, 1994]. The maps (not shown) show that, of all areas of the South Pacific, this region should be most favorable to salt fingering. Turner angles are calculated here also from the present CTD profiles using vertical gradients estimated from a straight line fit over 10 dbar. Along P19, Turner angles are just above 1.25 rad, hence marginally favorable for salt fingering, in the 40-50 m thick layer in the halocline centered at 200 dbar, at densities of 25.5 to up to 25.9 σ_θ (Plate 1). (When Turner angles are calculated over 4 dbar, they are much noisier but often exceed 1.25 within this layer.) Weak vertical steps of order 10 m thickness are found below the strongest part of the halocline on stations between 23°and 27°S (Plate 1). The weakness of the steps suggests either that salt fingering is not very active or that the high vertical stratification inhibits step formation.

Another possibility, suggested by the broad latitude range where Turner angles barely exceed 1.25 and also

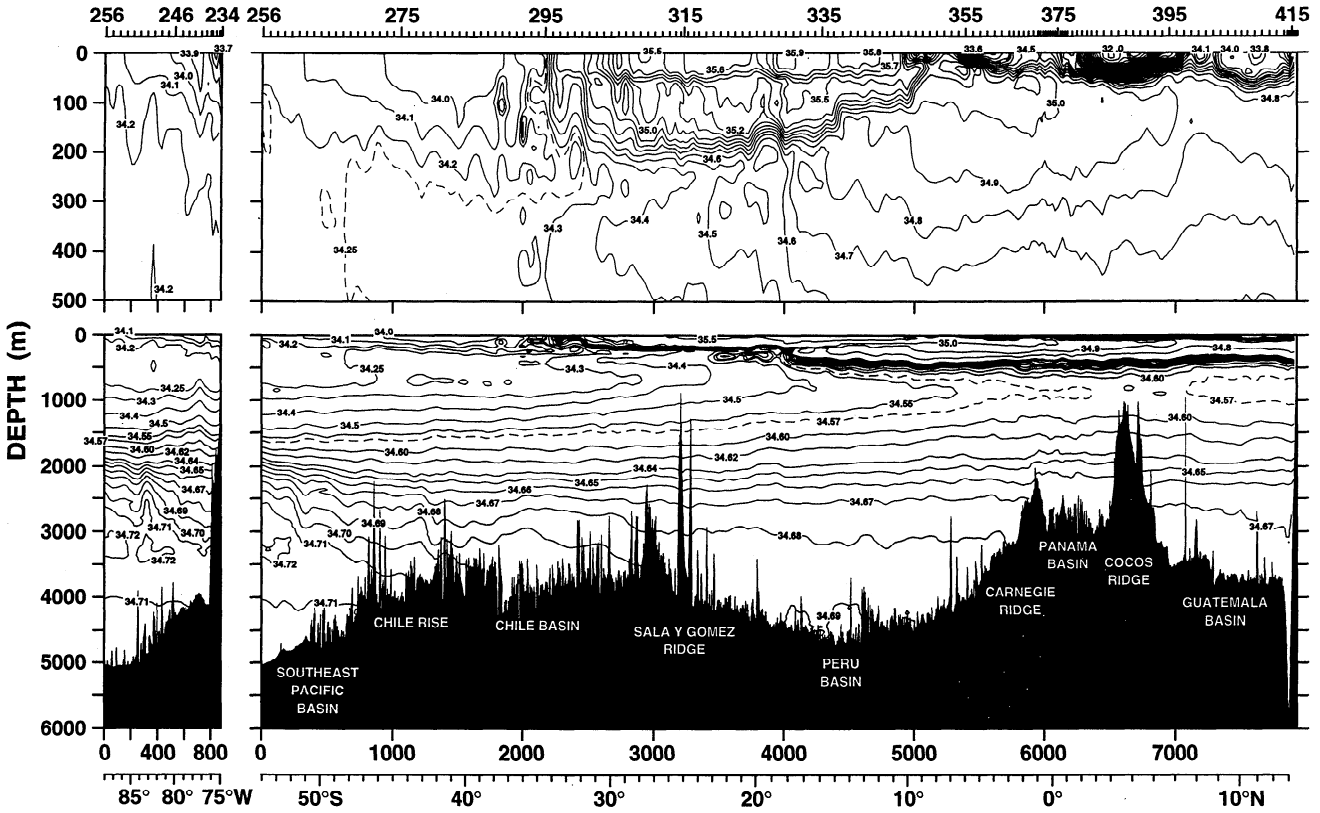

Figure 3. Salinity, based on CTD data, along the section shown in Figure 1.

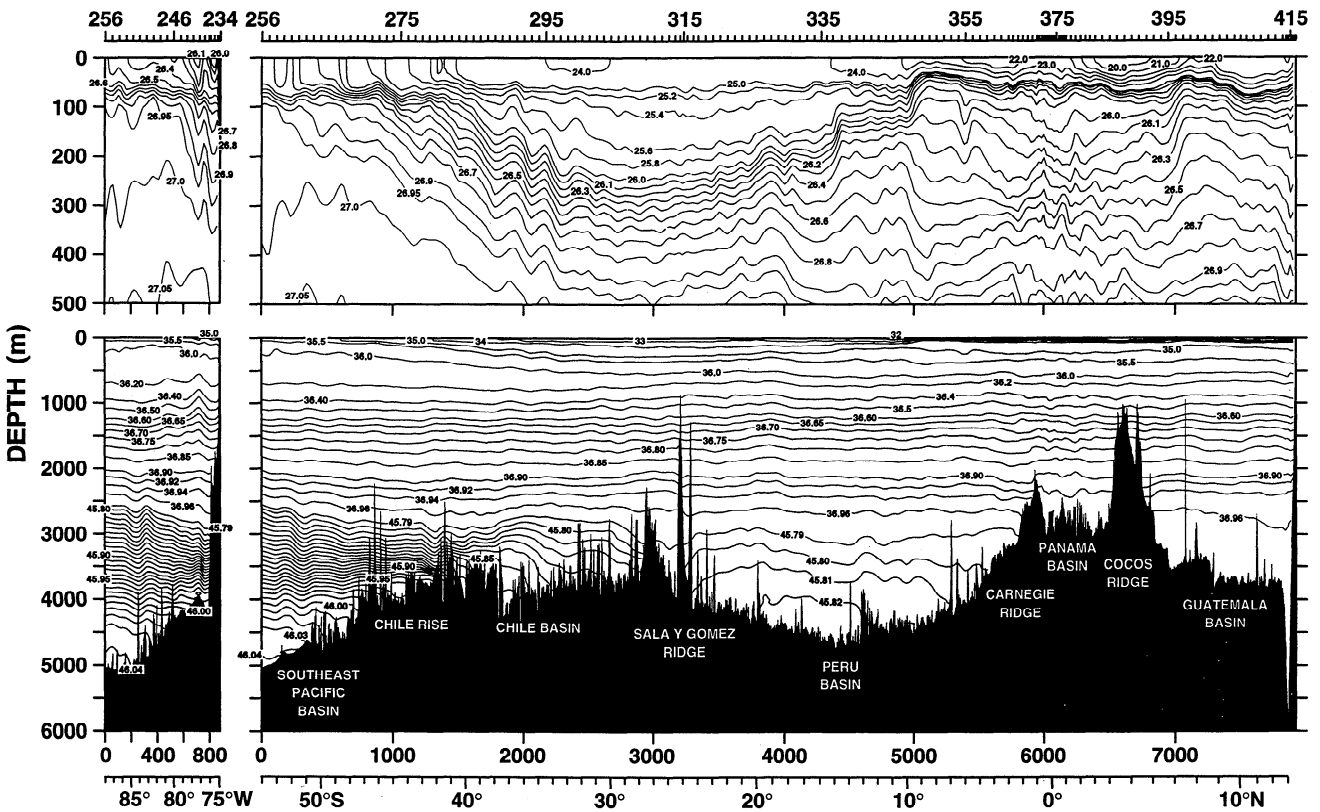

Figure 4. Potential density (kg m $^{-3}$), based on CTD data, along the section shown in Figure 1; (upper panels) value of σ_θ is shown, and (lower panels) value of σ_2 no greater than 36.96 kg m $^{-3}$ and σ_4 no smaller than 45.79 kg m $^{-3}$ is shown.

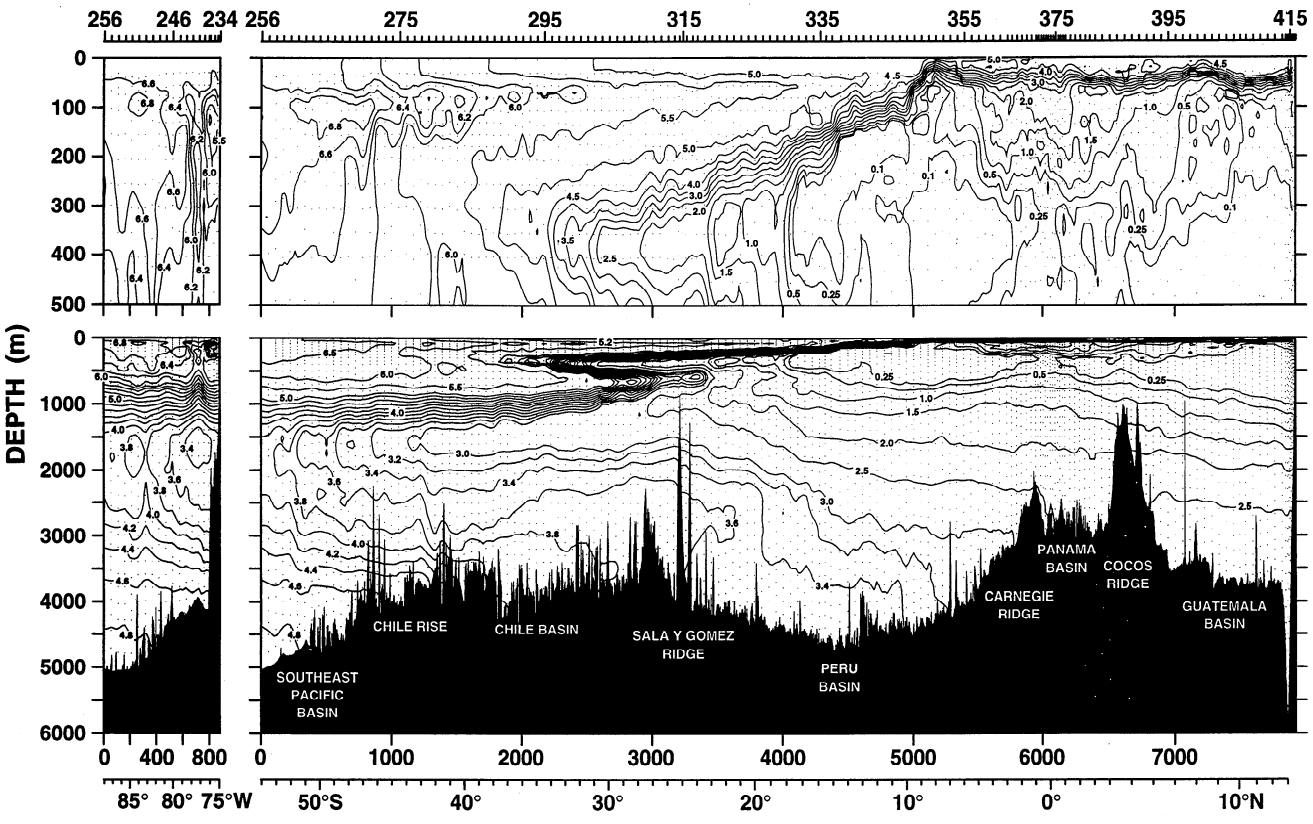

Figure 5. Oxygen (mL L^{-1}), based on bottle data, along the section shown in Figure 1.

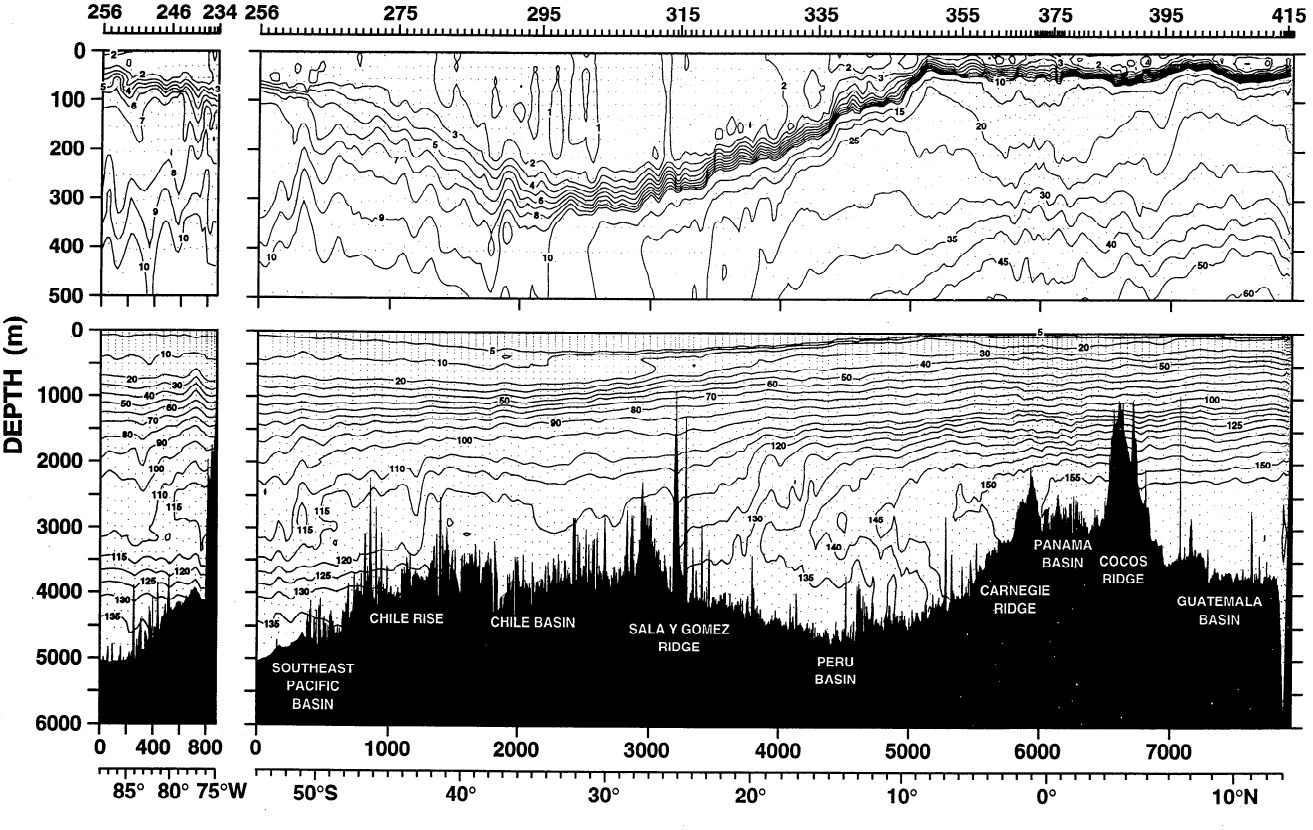

Figure 6. Silica (μmol kg^{-1}), based on bottle data, along the section shown in Figure 1.

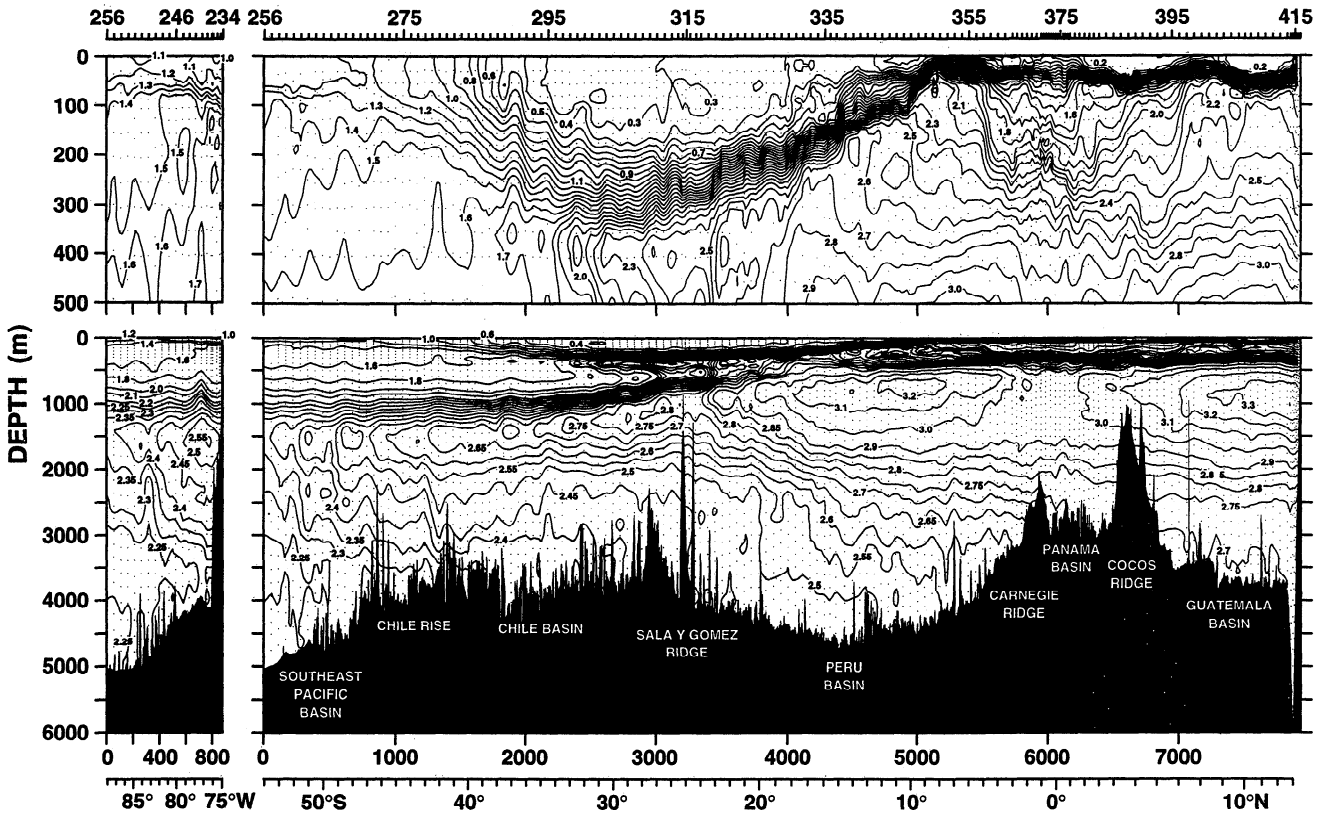

Figure 7. Phosphate (μmol kg^{-1}), based on bottle data, along the section shown in Figure 1.

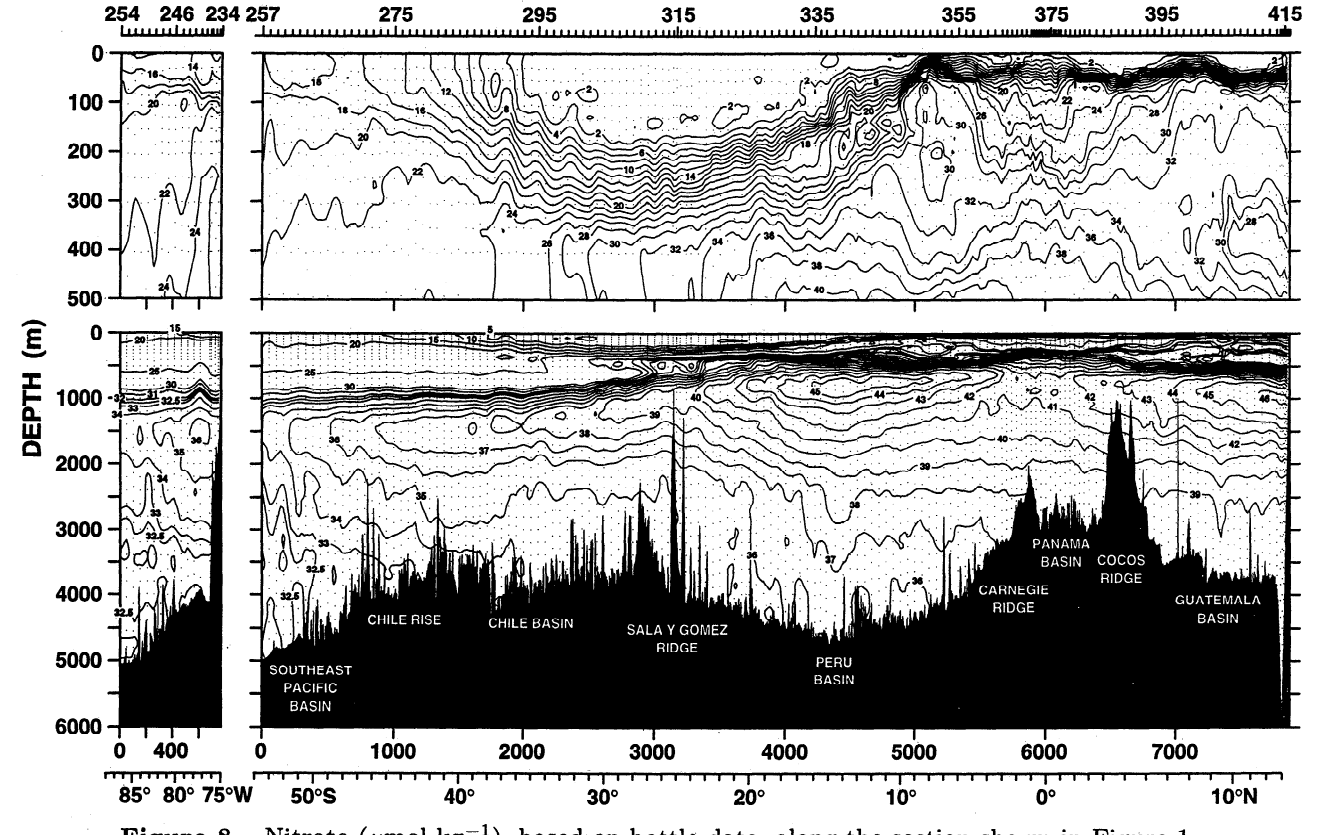

Figure 8. Nitrate (μmol kg^{-1}), based on bottle data, along the section shown in Figure 1.

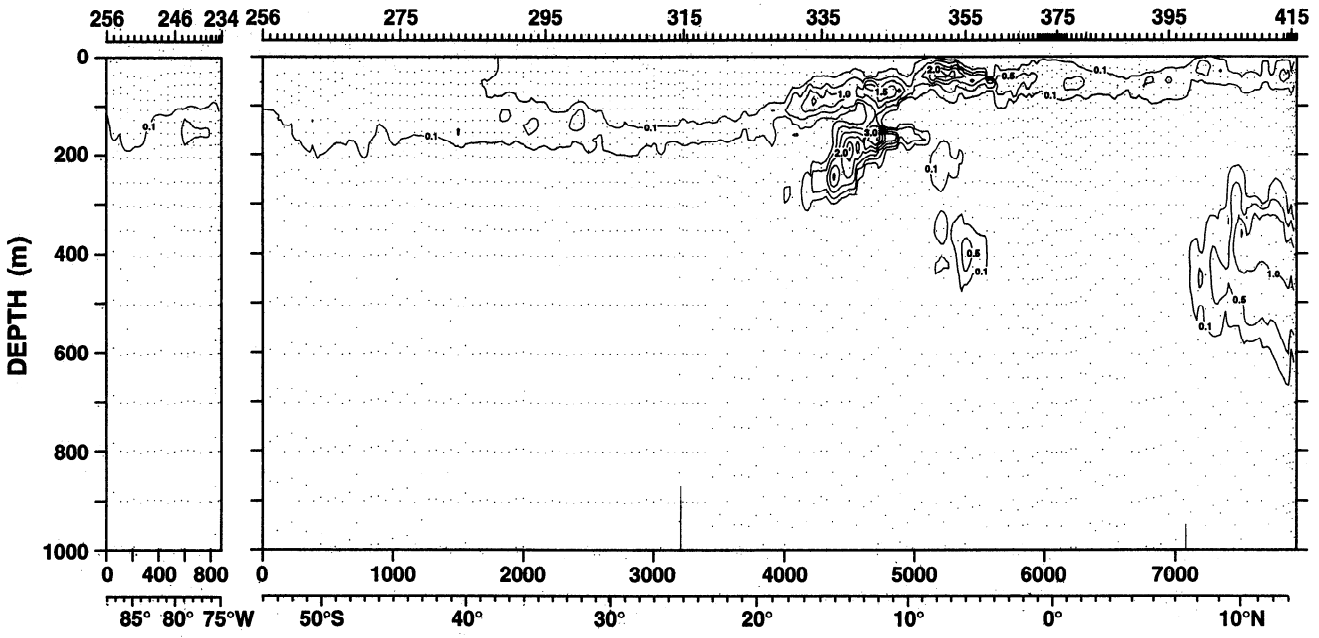

Figure 9. Nitrite (μmol kg^{-1}), based on bottle data, along the section shown in Figure 1.

by the observation of an even higher-salinity surface layer overlying the high-salinity pycnostad (Plate 1), is that the halocline centered at 200 dbar is not actively forced in this region during this season. Perhaps at the time when the halocline was being formed, salt fingering reduced the smoothed Turner angles to around 1.25, at which point the process ceased. Turner angles in the sharp halocline at the base of surface mixed layer (around 50 dbar), which one assumes is actively forced, also exceed 1.25 but are not useful for comparison since this transition layer is even thinner (order 10-20-m thick).

The subtropical water forms a thermostad embedded between the seasonal and permanent pycnoclines, thus between 50 and 200 m. The thermostad (also a pycnostad) is located between 33°and 15°S. It is centered at 25.5 σ_θ throughout the range, with temperature ~16°C in the south and rising to 18.5°C in the north and a concomitant change in salinity (Figure 12). This feature appears to be prevalent at the same latitudes east of 90°W [*Love*, 1972; *Tsubota*, 1973] but is not easily apparent in the historical data at and west of 95°W [*Stroup*, 1969, Figure 15; *Craig et al.*, 1981, Plate 25; *Tsuchiya and Talley*, 1996, Figure 2]. However, examination of the new WOCE section at 103°W (P18) shows a well-defined pycnostad at slightly lower density and higher temperature (25.3 σ_θ, 19°-21°C) than at 88°W. The zonal section at 28°S occupied in austral winter 1967 [*Reid*, 1973a] shows water of about these densities in the thick surface mixed layer. The WOCE section at 17°S occupied in March-April 1994 (M. S. McCartney, personal communication, 1997) skirts the northern side of the pycnostad but shows evidence of the 25.3 σ_θ pycnostad to 120°W with even weaker signatures as far as 140°W; east of 100°W the density rises to 25.6 σ_θ at 90°W, and the pycnostad disappears east of this.

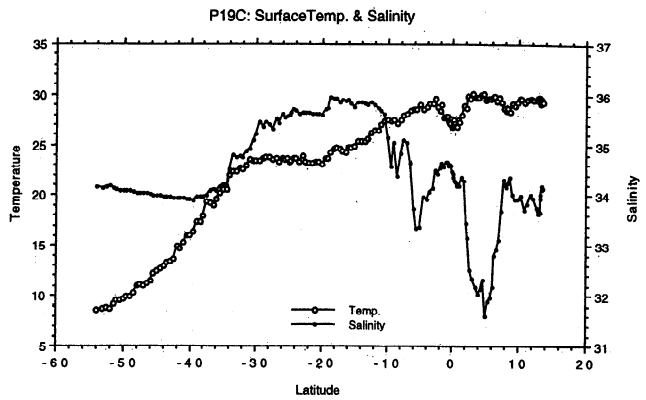

Figure 10. Sea surface temperature (degrees Celcius) and salinity, based on bottle measurements, along 88°W.

The pycnostad is apparently a remnant of the winter mixed layer in the eastern South Pacific north of the subtropical front [*Deacon*, 1982; *Stramma et al.*, 1995], which is the banded zone between 37°and 33°S on P19. North of the front, surface salinity is high (previous paragraphs), and winter mixed layers exceed 100-m thickness [*Wyrtki*, 1964b]. It is possible that the elevated salinities are responsible for the relative thickness of the winter layer. The long-term mean winter outcrops of the 17°-18°C isotherms are located near 24°-28°S at 88°W and farther north east of 88°W. Winter surface density is around 25.4 σ_θ over this fairly large region of the eastern subtropical gyre [*Levitus*, 1982]. The reduced density of the pycnostad toward the west and north reflects the winter density distribution.

This shallow pycnostad is analogous to a low-density pycnostad in the eastern subtropical North Pacific [*Talley*, 1988], also associated with subduction from a

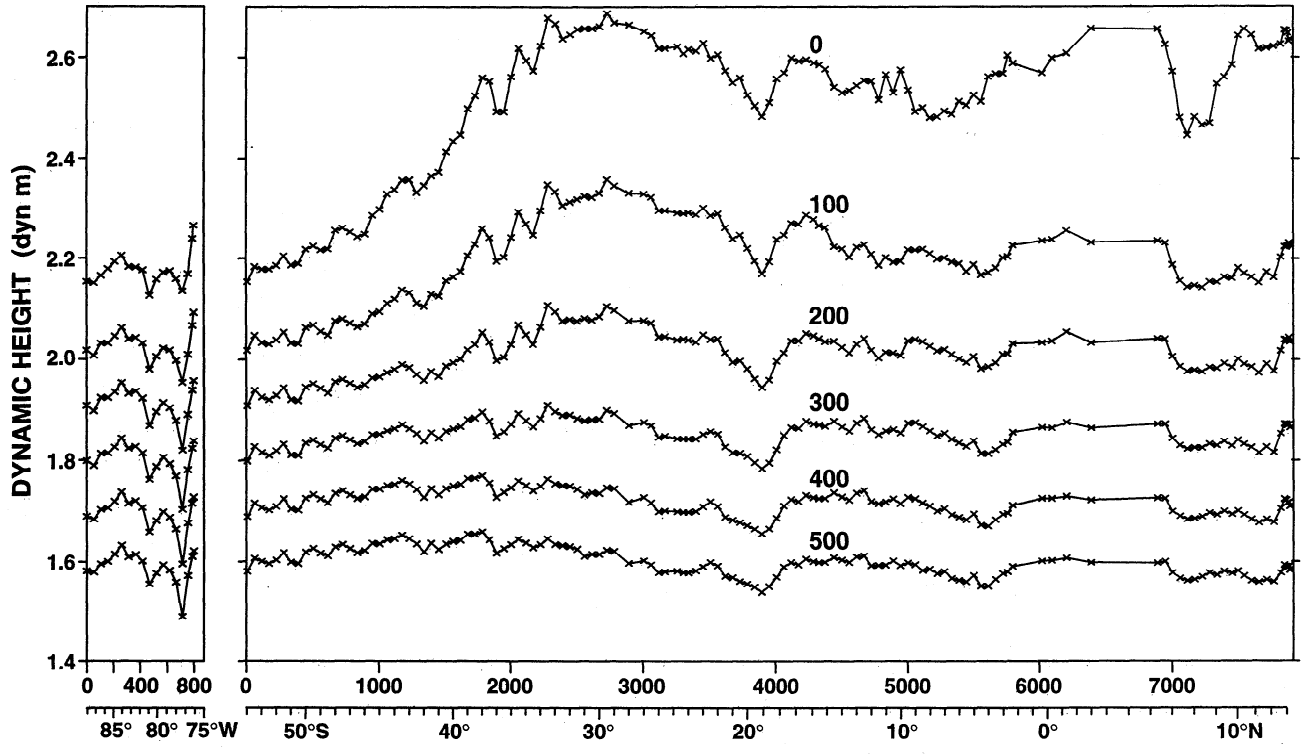

Figure 11. Profiles of steric height (dynamic meters = 10 m $^{-2}$ s $^{-2}$ of the 0-, 100-, 200-, 300-, 400-, and 500-dbar isobaric surfaces along the section shown in Figure 1. The reference pressure is 3000 dbar.

relatively thick surface layer; *Hautala and Roemmich* [1998] describe its properties in detail. Details of the South Pacific pycnostad properties, its relation to elevated surface salinity, and how much it reflects local winter properties as opposed to advected properties following subduction are being treated separately.

In the domain of the subtropical water, there is a shallow oxygen maximum (at 50-100 m), which appears to begin farther south and extends northward just beneath the seasonal thermocline in the thermostad region. The water at and above the maximum is supersaturated with oxygen. This excess oxygen is believed to arise from photosynthetic production of oxygen that remains trapped beneath the strong density gradient created by summer warming of near-surface water [*Shulenberger and Reid*, 1981].

The northern boundary (10°S) of the subtropical water at the sea surface is marked by a strong salinity front, across which salinity drops from 35.6 to 34.6 (see Figure 10). North of the front, the subtropical water extends under the low-salinity equatorial surface water and is recognized as a subsurface vertical maximum of salinity all the way to the northern end of the section. Near the front the maximum lies at 40-50 m (~25 σ_θ) in the pycnocline, but farther north, it gradually shifts to below the pycnocline reaching ~150 m (26.2 σ_θ) at 13°N just off the coast of Guatemala. The maximum shows isolated cores of laterally higher salinity at 1°-2.5°S and 6°-7.5°S. The former is due to eastward advection of high-salinity water in the Equatorial Undercurrent [*Lukas*, 1986]. The latter extends close to the sea surface to expose the lateral maximum at the surface. The significance of this feature is unclear, although the source of high salinity appears to be to the west of the section.

Near the southern boundary of the subtropical water, there are two salinity fronts at 30°and 34°S, across which the surface salinity decreases sharply southward. The surface temperature changes little across the northern front but shows a relatively strong gradient at the southern front. The subsurface isotherms at 100-500 m also exhibit a steeper northward downslope at the southern front. The close station spacing of our section resolves this frontal structure quite well, and we identify the southern front (at 34°S) as the subtropical front.

Between the subtropical front and 15°S and just below the subtropical water, there is a vertical minimum of salinity centered at 26.0-26.2 σ_θ (~250 m). This shallow salinity minimum in the eastern South Pacific has been documented by various investigators [e.g., *Reid*, 1965, 1973b; *Tsuchiya*, 1982]. On our salinity section (Figure 3) it appears to originate from low-salinity surface water south of the subtropical front at 34°S (described in the next paragraph as part of broad zonal low-salinity feature). The surface water density, however, is much lower than that of the salinity minimum. Nevertheless, it is possible that the surface water is cooled down in winter to become dense enough to be the source of the salinity minimum. This shallow salinity minimum as well as an analogous shallow minimum in the eastern North Pacific can be explained in the framework of the ventilated thermocline theory of *Luyten et al.*

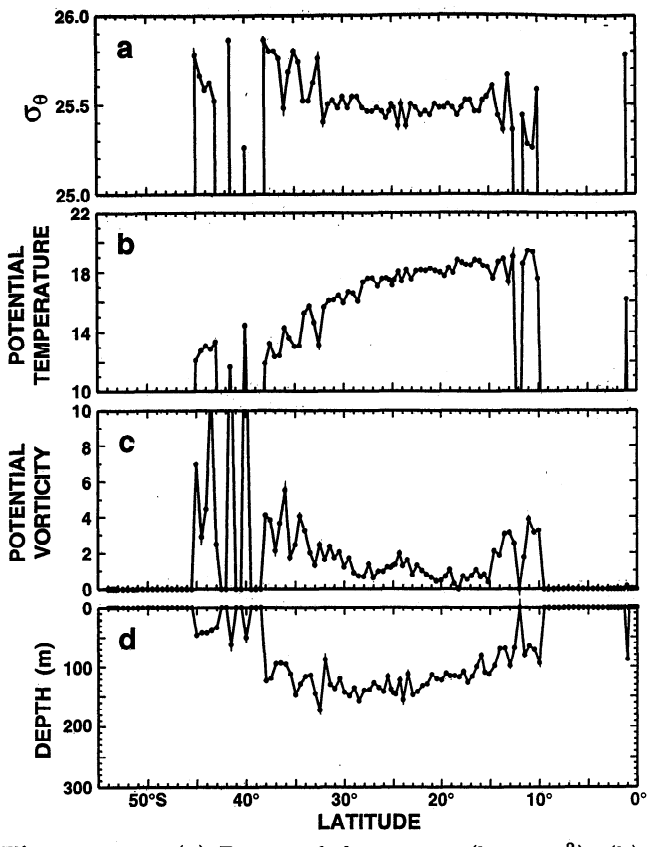

Figure 12. (a) Potential density σ_θ (kg m $^{-3}$), (b) potential temperature (degrees Celcius), (c) potential vorticity (10^{-12}cm^{-1}s^{-1}), and (d) depth (meters) at the vertical stability minimum between 25.2 and 25.9 σ_θ, characterizing the shallow pycnostad of the subtropical gyre; on the basis of the discrete bottle data with the potential vorticity calculation as described in the text.

[1983] as arising from subduction of low-salinity surface water from the south and east underneath the subtropical water by the wind-driven gyre circulation [*Talley*, 1985]. Subduction patterns in the South Pacific shown by *de Szoeke* [1987] indicate the plausibility of this mechanism.

South of the subtropical front, the surface salinity decreases more gradually to reach a minimum (~34.0) at 40°S and then increases again slowly southward. The surface temperature decreases almost steadily from 22°C at 34°S to below 9°C at 54°S, while the surface density increases from 24.0 to 26.5 σ_θ. This meridional minimum of salinity is of particular interest because the surface salinity in these latitudes decreases southward in most other areas around Antarctica. The minimum is clearly defined in prior data and is found to be associated with a tongue of low surface salinity extending westward from the coast of South America [e.g., *Schott*, 1935; *Sverdrup et al.*, 1942; *Reid*, 1969; *Levitus*, 1982]. This lower-salinity water is about 150-m thick and, as was noted just above, is the apparent source of the shallow salinity minimum in the eastern subtropical South Pacific, likely through subduction. *Deacon* [1977] reviewed evidence for the low-salinity tongue from various sources and argued for anticyclonic circulation in the upper 500 m of the eastern subantarctic Pacific Ocean, as postulated earlier by *McGinnis* [1974] from biological evidence. Deacon suggested a flow at 40°-45°S that carries fresh water from the heavy rainfall area along the coast of southern Chile westward to 130°W or possibly farther with a relatively strong eastward flow to the south of it. *Neshyba and Fonseca* [1980] presented additional data to suggest this westward flow in the low-salinity area, but the evidence remained inconclusive. They noted that the low-salinity tongue occurs in the area of high precipitation associated with the subpolar low-pressure belt but that the maximum precipitation is found well south of the axis of the tongue. Although the distribution of the sea surface steric height relative to 3000 dbar based on our individual station data exhibits narrow bands of westward flow near the northern edge of the tongue (Figure 11), meridionally smoothed geostrophic flow is dominantly eastward in the upper 300 m of the entire low-salinity area. In a short note, which will be published elsewhere, we map the near-surface salinity and present evidence that the low-salinity tongue arises from the strong eastward advection in the Antarctic Circumpolar Current region compared with the weaker eastward advection up the axis of the low-salinity tongue, both in the presence of a broad precipitation band, and not from westward advection as had been argued by *Deacon* [1977] and *Neshyba and Fonseca* [1980].

From station 256 eastward along 54°S, the surface temperature increases and the surface salinity decreases. Within about 200 km of the coast both isotherms and isohalines in the upper 300 m slope down sharply onshore, and between this slope and the coast is found a core of low-oxygen, high-nutrient water. This feature suggests the presence of a narrow poleward coastal flow (see also left panel in Figure 11).

3. Subpycnocline Waters

Within about 150 km of the Guatemalan coast, subpycnocline isopycnals generally descend toward the coast, suggesting a narrow poleward (northward) eastern boundary undercurrent. At 500-800 m this shoreward descending trend is disrupted by a sharp isopycnal ridge, which may indicate the presence of a small cyclonic subsurface eddy in the eastern boundary region.

Perhaps the most prominent feature of the property distribution in the water column immediately below the sharp equatorial pycnocline is a thick layer of extremely low oxygen centered roughly at 26.6-27.0 σ_θ). It is separated laterally into two domains by a band of laterally higher oxygen within a few degrees of the equator. The oxygen content is particularly low from 5°N to the coast of Guatemala in the northern domain and between 3°and 17.5°S in the south-

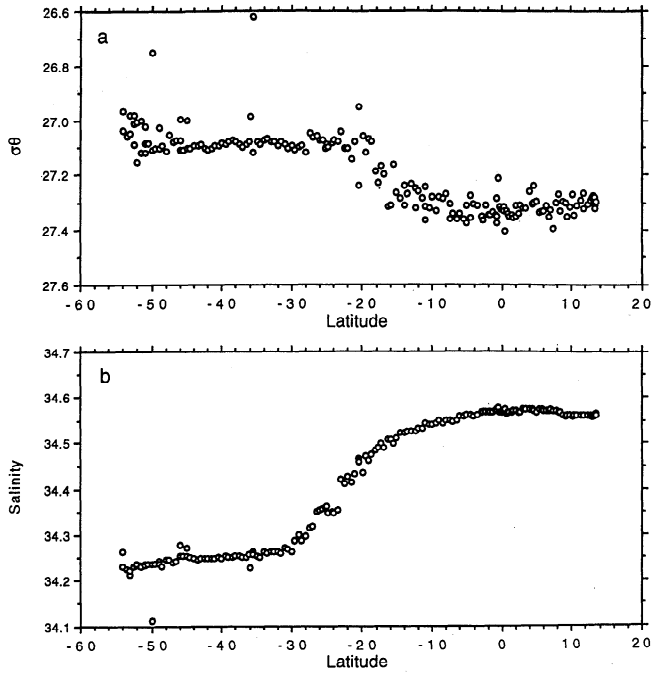

Figure 13. (a) Potential density σ_θ (kg m $^{-3}$) and (b) salinity at all salinity minima for σ_θ >26.6, based on bottle measurements, along 88°W.

ern domain, with the lowest values falling well below 0.1 mL L^{-1}. At ~18°S the southern low-oxygen domain is demarcated by a very sharp southward increase in oxygen (1 mL L^{-1} in 1°of latitude). These domains represent the well-known subpycnocline low-oxygen waters that extend westward on both sides of the equator from the coasts of Central and South America [*Bennett*, 1963; *Wooster and Cromwell*, 1958; *Knauss*, 1963; *Reid*, 1965] and have been accounted for as a consequence of minimal lateral replenishment [*Reid*, 1965] or as shadow zones unventilated by the wind-driven circulation [*Luyten et al.*, 1983]. Chlorofluorocarbon (CFC) saturations on P19, however, are up to 25% where oxygen saturations are as low as 5-10%, indicating that the low-oxygen layer is ventilated; the CFCs are being used to determine an oxygen utilization rate for this region [*Fine and Maillet*, 1994].

The low-oxygen domains in the equatorial region are accompanied by similar domains of high phosphate and nitrate, although their maxima are deeper than the oxygen minimum roughly by 500 m and lie in the depth range of the intermediate waters described in the next section. Unlike phosphate and nitrate, silica in these domains increases monotonically downward without exhibiting any extremum.

Near the coast of Central America north of 8°N the nitrate concentration shows a well-defined vertical minimum (< 28μmol kg^{-1}) centered at about 400 m (26.8 σ_θ). This distribution is peculiar in that the phosphate section does not reveal any analogous feature. The nitrate minimum is found to be coincident with a well-developed maximum of nitrite in the subpycnocline layer (Figure 9). This nitrite maximum is separate from a shallower primary maximum, which occurs in the pycnocline everywhere on the present section. The nitrate minimum and the deeper subpycnocline nitrite maximum are believed to be produced by denitrification of nitrate that takes place in extremely low oxygen water such as that found in the eastern tropical Pacific and the northern Arabian Sea [*Brandhorst*, 1959]. A similar but less-developed nitrate minimum is also observed at ~200 m near 8°S and ~150 m between 12°and 14°S in the corresponding low-oxygen domain south of the equator. Like the minimum in the northern hemisphere, this minimum is associated with a strongly developed secondary maximum of nitrite, as was also observed by many previous investigators [e.g., *Wooster et al.*, 1965].

The shallow salinity minimum at 15°-34°S (section 2) is underlain by a tongue of high salinity extending southward roughly along 26.4-26.8 σ_θ (300-500 m). South of ~25°S, this high-salinity tongue generally coincides with tongues of low oxygen, high phosphate, and high nitrate. Silica shows a weak maximum only near 25°-30°S at this depth. These extrema of the properties are more pronounced near the coast of South America, and *Wooster and Gilmartin* [1961] used the high-salinity, low-oxygen characteristics to track the flow of the poleward eastern boundary undercurrent (Peru-Chile Undercurrent) underneath the equatorward Peru Current. Although our section lies far offshore of the eastern boundary, the high-salinity, low-oxygen, high-nutrient water we observe on the section may derive its characteristics from the undercurrent water.

The Subantarctic Mode Water [*McCartney*, 1977, 1982] is clearly visible as a thick pycnostad spanning from 26.9 to 27.1 σ_θ and centered at about 27.05 σ_θ all along 54°S and as far north as 28°S along 88°W. At the base of the pycnostad is the salinity minimum of the Antarctic Intermediate Water located at 27.1 σ_θ (Figure 13). North of 48°S, the pycnostad contains an oxygen maximum, which underlies the low-oxygen tongue noted in the preceding paragraph and extends northward beyond the northern limit of the pycnostad. The Subantarctic Mode Water is recognized also as a thermostad developed at 5°-6°C. However, the thermostad fades out near 37°S and does not penetrate as far north as the pycnostad.

At station 242 (54°S, 77°W) on the bottom rise offshore of the Chile Trench a notable uplift of isopleths of all properties can be seen below the pycnocline down to 1500 m and may be interpreted to be a cyclonic eddy. Above ~1000 m the uplift of isopleths of oxygen, phosphate, and nitrate tends to exceed that of isopycnals, so that the water at the center of the uplift is appreciably lower in oxygen and higher in phosphate and nitrate than the surrounding waters on the same isopycnals. This isopycnal property anomaly suggests that the eddy was generated not locally but farther to the north.

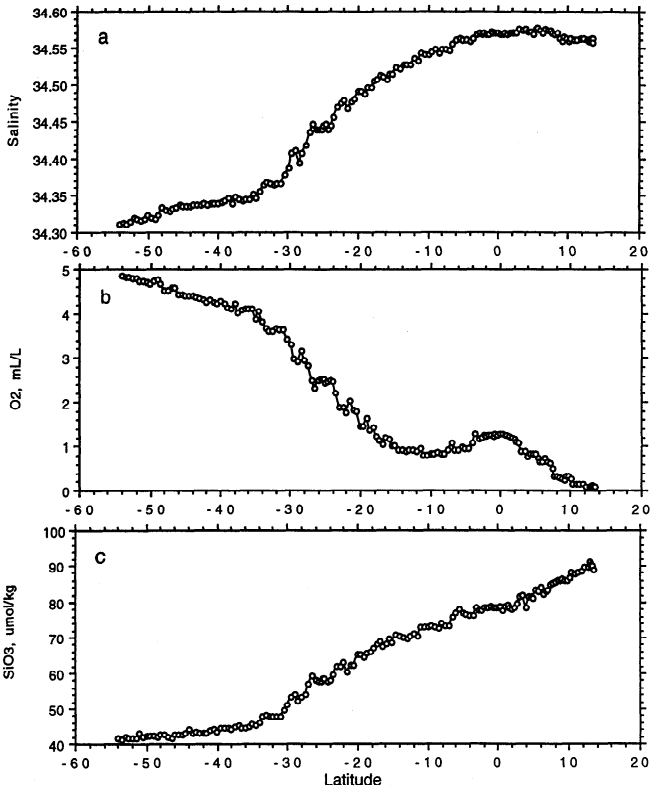

Figure 14. (a) Salinity, (b) oxygen (mL L^{-1}), and (c) silica (μmol kg^{-1}), at the 27.3 σ_θ isopycnal, based on bottle data, along 88°W.

4. Intermediate Waters

A vertical salinity minimum is present at 27.0-27.35 σ_θ (600-900 m) all along the 88°W section (Figure 13). On the basis of its density we identify the minimum with the Antarctic Intermediate Water [*Yuan and Talley*, 1992; *Talley*, 1993]. Because the minimum is only weakly defined south of ~50°S, it is not resolved by the isohalines in Figure 3. Most stations south of 50°S exhibit more than one minimum, which results in more scattered density values than at stations immediately to the north (Figure 13a). The core density (27.0-27.15 σ_θ) and salinity (~34.23) of the minimum in these high southern latitudes are similar to those of the Subantarctic Mode Water and are consistent with previous studies [*McCartney*, 1977, 1982; *Talley*, 1996a; M. McCartney and M. Baringer, personal communication, 1996] that suggested that at least part of the Antarctic Intermediate Water in the South Pacific subtropical gyre derives from the Subantarctic Mode Water formed off the west coast of southern Chile.

North of ~35°S, the salinity minimum is better defined; the Antarctic Intermediate Water can be recognized clearly at 700-900 m (27.10-27.35 σ_θ) as northward and southward dual tongues of low salinity meeting near 5°N, where its core salinity reaches a local maximum slightly in excess of 34.57 (Figure 3). There is a sharp transition in the core density from 27.1 σ_θ at 20°S to 27.3 σ_θ at 17°S. The core salinity also increases northward significantly in these latitudes, but the increase begins farther south from ~30°S (see also Figure 14a). On both sides of this transition zone are found waters whose density and salinity are uniform within each but quite distinct from each other. The characteristic density and salinity of the water on the south are 27.1 σ_θ and 34.25, and those on the north are 27.3 σ_θ and 34.57.

This distribution of the Antarctic Intermediate Water along our section, marked by dual tongues of low salinity with a local meridional salinity maximum at about 5°N and characterized by two distinctively separate water types, is very much similar to that observed at other longitudes in the Pacific Ocean. *Tsuchiya and Talley* [1996] described the distribution at 135°W in detail and suggested that the two types of the Antarctic Intermediate Water belong to the different ocean circulation regimes associated with the South Pacific subtropical gyre and the narrow alternating zonal flows in the equatorial region. The present data are entirely consistent with their interpretation.

There is one feature that is not quite obvious at 135°W but is evident at 85°W. It is a broad band (5°S-5°N) of high-oxygen water centered at the equator (Figure 14b). Similar bands of low phosphate and low nitrate can be seen at the equator (not shown), but silica does not show such a feature (Figure 14c). The high-oxygen, low-phosphate, and low-nitrate bands clearly reflect the strong contrast in concentrations of oxygen and the two nutrients between the eastward flowing water along the equator and the westward flowing water in the lower part of the oxygen-depleted domains on both sides of the equator in the far eastern Pacific.

5. Deep Waters

Below the salinity minimum of the Antarctic Intermediate Water, there are several vertical property extrema, which can be used to differentiate deep waters. As described below, some of these extrema are clearly seen in the vertical sections, but the others are not resolved by the chosen isopleths. The vertical distributions of properties below 2000 m are illustrated for individual stations representative of different basins (Figure 15).

5.1. Oxygen, Phosphate, and Nitrate Extrema

A marked property extremum in this depth range is the oxygen minimum in the southern half of the section. It is recognized in Figure 5 as a tongue of low oxygen, which appears to emanate from the deeper portion of the southern low-oxygen domain in the equatorial region (Figure 5). Near its beginning (~18°S) the tongue lies at 800 m with a density of 31.8 σ_1 (36.3 σ_2), but its depth and density increase to 1500 m and 32.2 σ_1 (36.7 σ_2) as it extends southward to 35°S; it continues farther south remaining at a fairly uniform depth

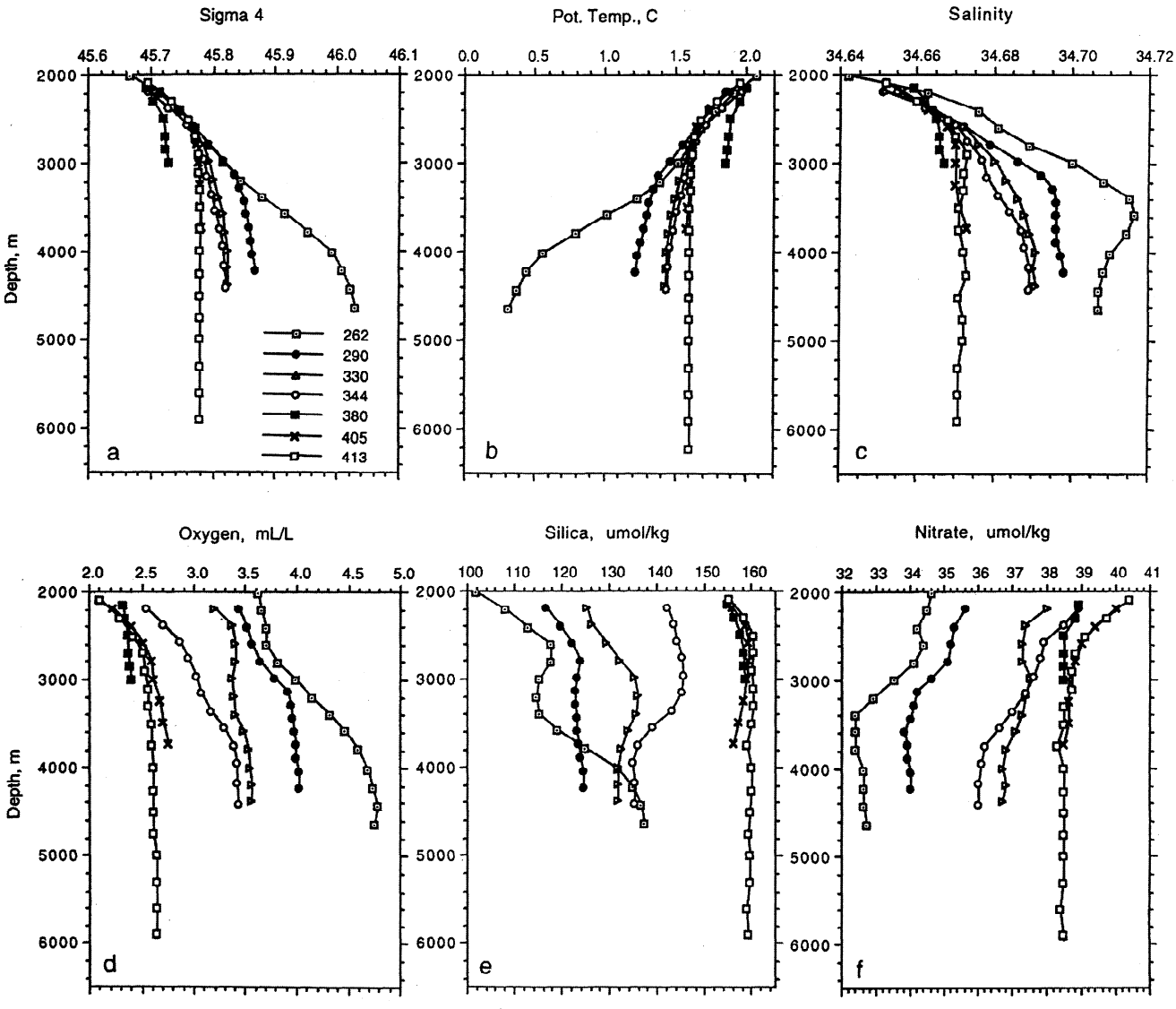

Figure 15. Vertical distributions of (a) potential density σ_4 (kg m $^{-3}$), (b) potential temperature (degrees Celcius), (c) salinity, (d) oxygen (mL L^{-1}), (e) silica (μmol kg^{-1}), and (f) nitrate (μmol kg^{-1}), below 2000 m in various basins. Station 262 is in the Southeast Pacific Basin, station 290 is in the Chile Basin, station 330 is in the southern Peru Basin, station 344 is in the northern Peru Basin, station 380 is in the Panama Basin, station 405 is in the Guatemala Basin, and station 413 is in the Middle America Trench.

(1700-1800 m) and density (32.3 σ_1, 36.8σ_2). Oxygen in the tongue increases from less than 1.5 mL L^{-1} at 18°S to above 3.8 mL L $^{-1}$ near the southern end of the 88°W section (Figure 5). Along 54°S, oxygen generally decreases toward the east to form an isolated core (< 3.4 mL L^{-1}) just off the coast of Chile, indicating that there is a band of lower oxygen along the coast. The low-oxygen tongue described above is accompanied by much similar but slightly shallower tongues of high phosphate and nitrate (Figures 7 and 8). These tongues appear to originate in the domain of high phosphate and nitrate south of the equator (section 3).

Reid's [1986, Figure 34] oxygen map for an isopycnal in the present density range reveals low-oxygen water extending southward all along the coast of South America. On the basis of this map and the silica distribution on the same isopycnal (his Figure 35) he suggested that water from the North Pacific crosses the equator at the eastern boundary, turns westward and then back eastward near 10°S, and extends southward along the eastern boundary of the South Pacific. He noted also that there is a substantial contribution of water to this eastern boundary flow from the eastern limb of the anticyclonic gyre of the subtropical South Pacific. More recently, he presented an additional discussion of the cross-equatorial flow path of the North Pacific water to the eastern boundary of the South Pacific [*Reid*, 1998]. Our data are used here to examine water properties along the 36.7σ_2, isopycnal, which is roughly coincident with the oxygen minimum south of

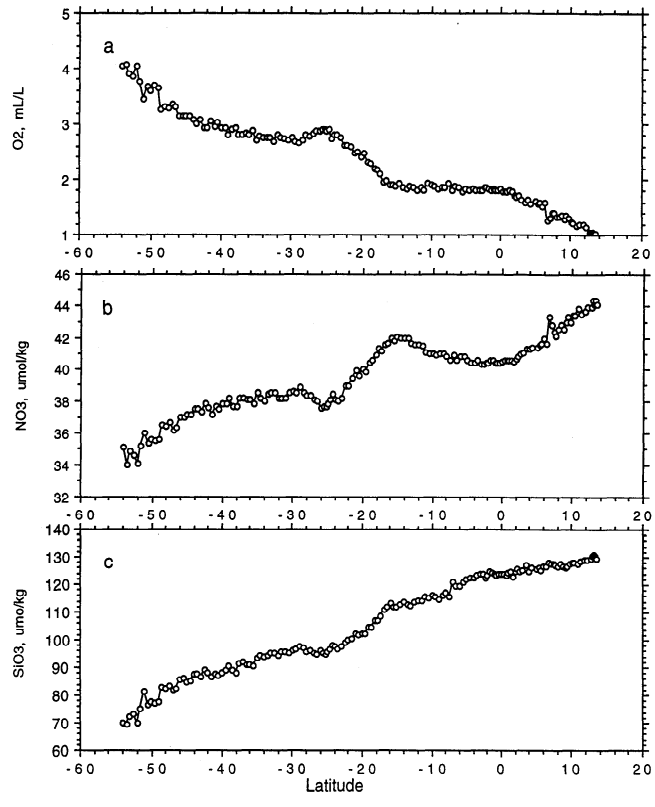

Figure 16. (a) Oxygen (mL L^{-1}), (b) nitrate (μmol kg^{-1}), and (c) silica (μmol kg^{-1}) at the 36.7 σ_2 isopycnal, based on bottle measurements, along 88°W. This isopycnal approximately coincides with the deep oxygen minimum south of about 30°S but lies well below the major oxygen minimum of the equatorial region.

about 30°S. Although oxygen shows a generally monotonic southward increase and silica shows a similar decrease in the equatorial region, a well-defined minimum of nitrate (phosphate also but not shown) is found at the equator (Figure 16). The equatorial minimum is accompanied by a maximum at 15°S. This distribution of nitrate (and phosphate) might indicate that high-nutrient (low-oxygen) water in the eastern North Pacific does not directly contribute to the high-nutrient (low-oxygen) water along the eastern boundary of the South Pacific.

In the vertical sections, middepth (1200-1800 m) isopleths of oxygen, phosphate, and nitrate exhibit a weak ridge and those of silica exhibit a slight trough at the crest of the Sala y Gomez Ridge (25°S), whereas isopycnals remain nearly level. Isopycnal property distributions (Figure 16) demonstrate the presence of a lateral maximum of oxygen and lateral minima of nutrients centered at 25°-26°S. The oxygen maximum and nutrient minima imply an eastward flow at these latitudes.

A core of high-oxygen water (> 3.6 mL L^{-1}) is found at ~2800 m (36.96 σ_2, 45.78 σ_4), on the northern flank of the Sala y Gomez Ridge (Figure 5). It has a vertical scale of 500 m and a horizontal scale of 500 km. The significant dip of the isopycnals for 45.79-45.81 σ_4 toward the ridge in this area indicates that the geostrophic flow relative to the bottom is westward and its maximum speed occurs at about the depth of the high-oxygen core, where isopycnals are nearly horizontal (Figure 4). This high-oxygen water is evidently derived from the Chile Basin through gaps of the Sala y Gomez Ridge. Similar cores of low phosphate and nitrate are found at the same location north of the ridge, but they are not resolved by the choice of the isopleths in Figures 7 and 8.

Weak minima of phosphate and nitrate exist above the bottom of the Southeast Pacific Basin. They are discussed below in connection with a salinity maximum associated with them.

5.2. Salinity and Silica Extrema

A broad but clear salinity maximum (>34.71) occurs at 37.05-37.09 σ_2 (45.88-45.94 σ_4) in the Southeast Pacific Basin (Figures 3 and 15c). The highest salinities (>34.72) are observed at 3300 m near the southern end of the 88°W section, and the maximum deepens toward the north to 3800 m at 47°S, where it intersects the bottom. This salinity maximum roughly coincides with broad and weak minima of phosphate and nitrate, which are discernible by the isopleths for 2.25 (phosphate) and 32.5 (nitrate) μmol kg^{-1} (Figures 7 and 8; see also station 262 in Figure 15f). About 500 m above the salinity maximum, there is a silica minimum at 37.00-37.04σ_2, (45.80-45.85 σ_4, 2800-3300 m). Although this silica minimum is revealed by the 115 μmol kg^{-1} isopleths only near the coast of southern Chile (Figure 6), it is present on almost all stations along 54°S and as far north as the Chile Rise along 88°W; furthermore, a few stations in the southern Chile Basin show its last vestige (see station 290 in Figure 15e). This deep water containing the salinity maximum, phosphate and nitrate minima, and silica minimum at somewhat different levels obviously has its origin in remote sources in the North Atlantic but still preserves the North Atlantic signatures when it reaches our section in the form of the Upper Circumpolar Water after a long journey from the North Atlantic.

The silica minimum is necessarily overlain by a silica maximum at about 2700 m (36.96-36.98 σ_2, 45.78-45.80 σ_4), but it cannot be seen in Figure 6 except near the coast of southern Chile at 54°S. A more extensive and clearly defined silica maximum occurs at middepth in the Peru Basin. In Figure 6 it is recognized as a thick tongue lying at 2500-3000 m (36.96-36.99 σ_2, 45.76-45.80 σ_4), from the southern flank of the Carnegie Ridge (2°S) as far south as 19°S. Another deep silica maximum is weakly developed above the bottom nearly everywhere in the Guatemala Basin (not revealed in Figure 6; see station 405 in Figure 15e). It occurs near 2800 m at a density of ~36.96 σ_2. These three silica maxima observed at separate locations on our section have about the same core den-

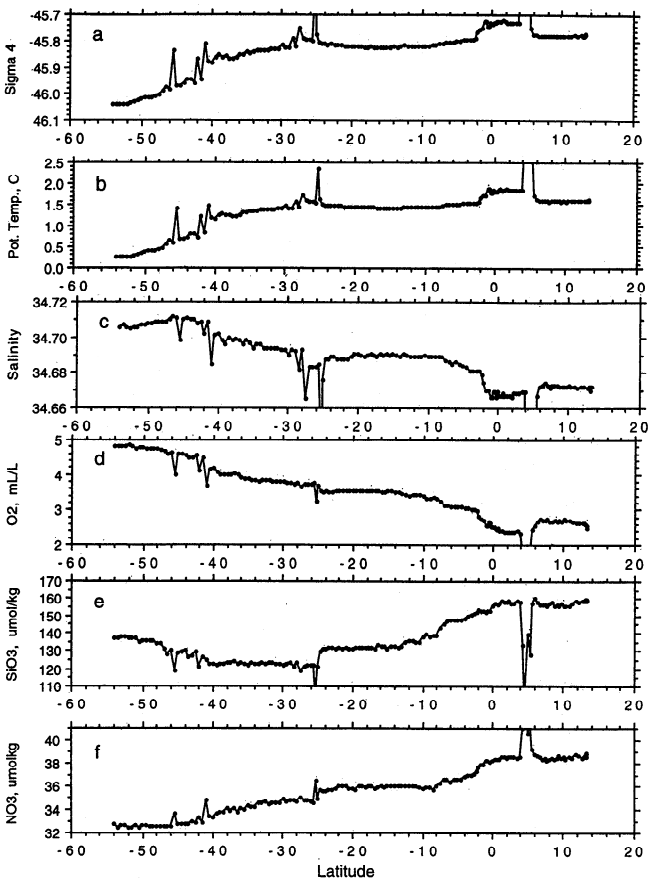

Figure 17. Properties at the deepest bottle along 88°W from station 256 (54°S) off southern Chile northward to station 417 (13.3°N) on the inshore slope of the Middle America Trench off Guatemala. (a) Potential density σ_4 (kg m $^{-3}$), (b) potential temperature (degrees Celcius), (c) salinity, (d) oxygen (mL L^{-1}), (e) silica (μmol kg^{-1}), and (f) nitrate (μmol kg^{-1}). Stations 418-422 at the northern end of the section are shallower than 2000 m and not included in the figure. Some properties are off scale over the crests of the Sala y Gomez Ridge (25°S) and the Cocos Ridge (5°N).

sity and appear to represent the southeastern edge of the well-known oceanwide deep silica maximum in the Pacific, which has been illustrated, for example, in a Geochemical Ocean Sections Study (GEOSECS) atlas [*Craig et al.*,1981] and more recent high-resolution vertical sections by *Roemmich et al.* [1991], *Talley et al.* [1991], *Tsuchiya and Talley* [1996], and *Wijffels et al.* [1996], and which has been studied by many investigators [e.g., *Edmond et al.*, 1979; *Talley and Joyce*, 1992]. The southward extension of this high-silica water from the North to the South Pacific along the west coast of South America is apparent on a middepth isopycnal map of silica presented by *Reid* [1981].

6. Bottom Waters

Our section transects five major deep basins (Southeast Pacific, Chile, Peru, Panama, and Guatemala basins) east of the East Pacific Rise and provides an excellent data set to study the bottom waters of these basins.

6.1. Southeast Pacific Basin

The south end of the 88°W section (station 256) is close to the northeastern edge of the Southeast Pacific Basin, but the water depth still exceeds 5000 m. The bottom water here is directly from the Lower Circumpolar Water of the Antarctic Circumpolar Current [e.g., *Warren*, 1973; *Mantyla*, 1975; *Mantyla and Reid*, 1983]. It is colder, denser, fresher, and higher in oxygen and silica than the overlying deep water characterized by the weak salinity maximum and silica minimum derived from the North Atlantic Deep Water (section 5). It is bounded on the top by a stronger vertical gradient of temperature centered at about 1°C (3500 m) (Figure 15b). This cold bottom water is blocked by the Chile Rise and extends only to 47°S on the southern flank of the rise, where the salinity maximum intersects the bottom. The bottom water characteristics near the southern end of the section (54°S) are typically $\theta \sim 0.24$°C, $S \sim 34.706$, $\sigma_4 \sim 46.04$, and $O_2 \sim 4.83$ mL L^{-1} with weak trends for northward increases in temperature and salinity and decreases in density and oxygen (Figure 17). These trends are associated to a large extent with the northward decrease in the bottom depth, but the temperature increase and the density (σ_4) decrease are associated also with the northward deepening of deep isotherms and isopycnals just south of the Chile Rise. The deepening of the isopycnals may be associated with an eastward geostrophic flow across the basin. The geostrophic circulation pattern of the near-bottom water deduced by *Reid* [1986, Figures 67 and 68; 1998, Figure 5k] from meager data in the Southeast Pacific Basin shows a cyclonic gyre with its eastward flowing northern limb on the southern flank of the Rise.

6.2. Chile Basin

North of the Chile Rise, our 88°W section traverses the westernmost portion of the Chile Basin, where the average depth is only about 3800 m. In all basins north of the Chile Rise the salinity maximum occurs at the bottom, and there is no such strong vertical gradient of temperature as that observed at the top of the bottom water in the Southeast Pacific Basin. Thus a relatively thick layer of fairly uniform characteristics develops just above the bottom (Figure 15).

As in the Southeast Pacific Basin, the bottom temperature increases northward (1.23°to 1.43°C) across the Chile Basin, but the salinity decreases northward (34.699 to 34.692), as do the density and oxygen (45.86 to 45.82 σ_4; 4.15 to 3.80 mL L^{-1}) (Figure 17). These changes are associated with a northward deepening of deep isopleths as clearly recognized in the vertical sections (Figures 2-5), and the slope of deep isopycnals, in particular, indicates an eastward geostrophic flow relative to the bottom. Such isopycnal slopes are typical of

most deep basins, except near strong western boundary currents and the Antarctic Circumpolar Current [*Talley*, 1996b]. It can be seen on *Reid's* [1986, Figure 58; 1998, Figure 5j] maps of adjusted steric height at 3500 dbar that the cyclonic gyre we have seen at greater depths in the Southeast Pacific Basin expands northward to cover the major part of the Chile Basin with an eastward flow representing the northern limb of the gyre.

Lonsdale [1976] showed that the primary source of the bottom water in the main portion of the Chile Basin (>4000 m) to the east of the present section is Southeast Pacific Basin water that leaks through the Valdivia Fracture Zone (3900 m), which intersects the Chile Rise at 41°S. However, the bottom water we observed along the western edge of the Chile Basin appears to be derived from shallower water above the crest of the rise; water characteristics much similar to those quoted above for the Chile Basin bottom water are found at 3200-3400 m near 41°S.

6.3. Peru Basin

Lonsdale [1976] suggested that the Peru Basin receives its bottom water from the Chile Basin by way of two separate routes: one route is through the narrow passage (4900 m deep) along the Peru-Chile Trench at the northeast end of the Nazca Ridge, and the other is through the shallower, broader sill (3900 m deep) between the Nazca and Sala y Gomez ridges. Our section passes just west of this broad sill partially obstructed by numerous seamounts and extends northward across the Peru Basin. It can be seen in Figures 2-8 and 17 that in the southern half of the Peru Basin, bottom water characteristics are relatively uniform at $\theta \sim 1.45$°C, S~34.689, σ_4 ~45.82, O_2 ~3.50 mL L^{-1}, SiO_3 ~131 μmol kg^{-1}, PO_4~2.49 μmol kg^{-1}, and NO_3 ~36 μmol kg^{-1}. An updated map of potential density (σ_4) at the bottom of the Pacific indicates that the bottom water here with σ_4 greater than 45.82 is supplied through the Peru-Chile Trench (A. W. Mantyla, personal communication, 1997). However, the lack of stations in the broader passage between the Nazca and Sala y Gomez ridges does not preclude the possibility that it can also be supplied through this passage. The near-bottom isopycnals for 45.79-45.81 σ_4 show a significant southward downslope on the northern flank of the Sala y Gomez Ridge and suggest a westward flow (relative to the bottom) of the near-bottom water that has entered the Peru Basin from the south. This water is clearly distinguished by its lower oxygen (3.50-3.55 mL L^{-1}) from the overlying higher-oxygen water (>3.6 mL L^{-1}, which is also flowing westward (section 5.1).

In the northern half of the Peru Basin, temperature, salinity, and density (σ_4) remain fairly uniform with values at about the same levels as those in the southern half. In contrast, the nonconservative properties show considerable north-south gradients; oxygen decreases and nutrients increase northward. The bottom water in the northern Peru Basin may have taken a more devious route either from the broader sill or from the narrow passage at the northeast end of the Nazca Ridge. The longer route to the northern basin can account for the lower oxygen and higher nutrients there. Although the weak northward deepening trend of the isopycnals for 45.80 and 45.81 σ_4 in the northern basin is suggestive of an eastward flow (Figure 4), the horizontal density gradient is too weak to infer the sense of the deep geostrophic flow with any confidence.

6.4. Panama Basin

The northward spreading of water continues from the Peru Basin into the bottom of the Panama Basin through the narrow gap (2900 m deep) situated between the Carnegie Ridge and the Ecuadorian coast and connecting the Colombian Trench in the Panama Basin with the Peru-Chile Trench to the south [*Laird*, 1971; *Lonsdale*, 1976]. From the distributions of temperature, salinity, and oxygen in the deep Panama Basin, *Laird* [1971] concluded that this gap is the only source of the near-bottom water in the basin and deduced abyssal flow paths that are consistent with the observed patterns of the properties. *Lonsdale and Malfait* [1974] presented geological evidence of an additional northward inflow to the Panama Basin through a saddle (~2300 m) near the middle of the Carnegie Ridge. Both *Laird* [1971] and *Lonsdale* [1976] noted the importance of geothermal heating in the modification and renewal of the bottom water. Our section passes right through this saddle (86°W) and grazes the western edge of the Panama Basin before turning to the northwest at the southern flank of the Cocos Ridge. The section shows laterally uniform characteristics (θ = 1.82°-1.85°C, S =34.667-34.669, σ_2 = 36.93, σ_4 = 45.73), except for the northward decreasing trend of oxygen (2.50 to 2.35 mL L^{-1}) (Figure 17). This bottom water in the western Panama Basin is somewhat warmer, fresher, and lower in oxygen than that observed farther to the east by *Laird* [1971]. The vertical sections (Figures 2-5, 7, and 8) suggest that it can be supplied from the south through the saddle of the Carnegie Ridge, but its high silica values (> 155 μmol kg^{-1}) are difficult to explain by this source (Figure 6).

6.5. Guatemala Basin

The Guatemala Basin is separated from the Panama Basin by the Cocos Ridge. It is bounded on the south by the Colon Ridge and on the west by the East Pacific Rise. Its bottom water is homogeneous in temperature, salinity, and density (σ_4) not only laterally but vertically up to ~2700 m (Figures 2-4 and 15). As can be seen clearly in the vertical sections and in Figure 17, it is colder (1.58°C), more saline (34.673), denser (36.97 σ_2, 45.78 σ_4), and higher in oxygen (2.65-2.75 mL L^{-1}) than any water in the Panama Basin. These

characteristics indicate that no inflow takes place from the Panama Basin to the Guatemala Basin to supply its bottom water. *Mantyla* [1975] suggested that the bottom water in the Guatemala Basin comes from the west crossing the East Pacific Rise at two different locations: the Siqueiros Fracture Zone (8°N) and, more likely, near the western edge of the Colon Ridge (2°N). He also noted two vertical minima of in situ temperature at 2600 and 3100 m in the Guatemala Basin and attributed them to these two sources with different sill depths. Our data, however, show only one in situ temperature minimum at 2700-2900 m on all stations in the Guatemala Basin; no indication can be found of a deeper secondary minimum with such a magnitude and on such a vertical scale as those illustrated by Mantyla. On the basis of more recent data taken along 10°N, *Wijffels et al.* [1996 p. 516] noted that the waters at depth in the Guatemala Basin are higher in salinity and lower in oxygen than those west of the East Pacific Rise at similar temperatures and suggested that the Guatemala Basin waters are "the product of slow warming by either downward heat diffusion or geothermal conduction." Additional hydrographic and bathymetric data are required to determine the source (or sources) of the Guatemala Basin bottom water.

The Middle America Trench, whose depth exceeds 6000 m on the present section, is filled with highly homogeneous water below about 3800 m (Figure 15). Its temperature, salinity, and density are much the same as those of the bottom water found elsewhere in the Guatemala Basin (Figure 17).

7. Summary and Discussion

The near-surface waters we find along the section are the following: a thin layer of the warm, very fresh equatorial surface water in the heavy rainfall area associated with the Intertropical Convergence Zone; the relatively warm, highly saline subtropical water produced by excess evaporation over precipitation; and the cool, fresh surface water in the heavy rainfall area in the subantarctic zone off southern Chile. The equatorial surface water occurs principally north of the equator, but part of it appears to have crossed the equator somewhere east of the section and is found near 5°S at 86°W. In addition, the colder, more saline thermocline water is exposed at the equator and near 8°N (Costa Rica Dome), where the upper portion of the thermocline rises to the sea surface. The boundaries between these waters found at the sea surface are marked by a strong gradient of salinity or strong gradients of both salinity and temperature. For example, the boundary between the equatorial surface water north of the equator and the upwelled thermocline water at the equator is the equatorial front described by *Wooster* [1969].

The subtropical water is developed down to 200 m between 10°and 34°S. The strong vertical gradients of salinity and temperature at the base of this thick layer indicate that salt fingering may possibly be an important mechanism to transfer salt downward. The subtropical water contains a thermostad (pycnostad) at 16°-18.5°C (25.5 σ_θ). It is analogous to a low-density pycnostad in the eastern North Pacific and is apparently a remnant of the winter mixed layer in the eastern South Pacific north of the subtropical front. Immediately below the seasonal thermocline, which defines the top of the thermostad, there is a vertical maximum of oxygen. It can be recognized as a northward high-oxygen tongue at 50-100 m, but the tongue begins far south of the thermostad region. North of 10°S, the subtropical water extends beneath the low-salinity equatorial surface water. It forms a vertical salinity maximum, whose density increases toward the north end of the section (from 25 to 26.2 σ_θ). This high-salinity water has isolated cores of laterally higher salinity at 1°-2.5°S and 6°-7.5°S. The former is associated with the Equatorial Undercurrent. The significance of the latter is not immediately clear, but previous studies based on the property distributions at the same longitude showed the presence of a subpycnocline eastward flow at 5.5°-7°S and identified it as the subsurface South Equatorial Countercurrent [*Tsuchiya*, 1975, 1985].

The low-salinity surface water in the subantarctic zone west of southern Chile attracted the attention of previous investigators, because it contrasts with the general southward decrease in the surface salinity for the most part of the Antarctic Circumpolar Ocean and because the observed westward extension of the low-salinity water from the coast of Chile suggests the presence of a westward flow against the strongly eastward background flow (West Wind Drift). With our data the low-salinity water is clearly defined in the upper 150 m between 35°and 50°S and is believed to be the source of the shallow salinity minimum in the eastern subtropical South Pacific. Our data, however, do not show evidence of westward surface geostrophic flow in these latitudes.

The well-known low-oxygen domains on both sides of the equator are the most dominant feature of the property distribution in the layer immediately below the sharp equatorial pycnocline. The oxygen content is particularly low from 5°N to the coast of Guatemala and from 3°S to 17.5°S, reaching well below 0.1 mL L^{-1}. The low-oxygen domains are accompanied by similar domains of high phosphate and nitrate, but their maxima are deeper than the oxygen minimum by 500 m. Silica does not show any extremum in these domains.

North of 8°N in the northern low-oxygen domain, nitrate shows a well-defined vertical minimum at about 400 m, which is not accompanied by a similar minimum in phosphate. The nitrate minimum is coincident with a well-developed nitrite maximum. The nitrate minimum and the nitrite maximum are believed to be a result of denitrification of nitrate. From our data we estimate that the decrease in nitrate at the core of the nitrate minimum is nearly 6 μmol kg^{-1}, while the corresponding increase in nitrite (i.e., maximum nitrite) is

only ~1.4 μmol kg^{-1}. Thus, if the vertical distribution of nitrate and nitrite is determined locally, further denitrification to gaseous nitrogen compounds may have occurred [*Thomas*, 1966]. A similar nitrate minimum and a corresponding nitrite maximum are found also in the low-oxygen domain south of the equator.

A tongue of high salinity extends southward from 15°to 34°S nearly along 26.4-26.8 σ_θ (300-500 m) just below the shallow salinity minimum. South of 25°S, the high-salinity tongue is generally coincident with tongues of low oxygen and high phosphate and nitrate. These tongues represent the subpycnocline water that is transported from the north by the poleward Peru-Chile Undercurrent along the coast of South America.

The Subantarctic Mode Water is well defined as a thick pycnostad at 26.9 to 27.1 σ_θ from the south end of the section as far north as 28°S. It is recognized also as a thermostad developed at 5°-6°C, but the thermostad does not extend as far north as the pycnostad. The Subantarctic Mode Water contains an oxygen maximum north of 48°S, and at the base of the Mode Water is found the salinity minimum of the Antarctic Intermediate Water.

The Antarctic Intermediate Water is present at 600-900 m all along the section. South of ~50°S, although its salinity minimum is only weakly defined, the core density (27.0-27.15 σ_θ) and salinity (~34.23) of the minimum are similar to those of the Subantarctic Mode Water, suggesting that at least part of the Antarctic Intermediate Water in the South Pacific subtropical gyre derives from the Mode Water formed off the west coast of southern Chile. North of ~35°S, the minimum is recognized clearly at 700-900 m as dual tongues of low salinity extending in opposite directions and meeting near 5°N, where the core salinity reaches a meridional maximum. The density of the salinity minimum increases rapidly from 20°to 17°S. The minimum salinity also increases northward significantly in this latitude range, but the increase begins farther south from ~30°S. The characteristic density and salinity at the salinity minimum are 27.1 σ_θ and 34.25 south of this transition zone and 27.3 σ_θ and 34.57 north of it. The former type of the Antarctic Intermediate Water is confined in the South Pacific subtropical gyre, and the latter type is found in the region of the equatorial zonal currents. This transition from one regime of circulation to another is clearly indicated by a local minimum of steric height at 19°S of upper layer isobaric surfaces (Figure 11).

Along the 36.7 σ_2 isopycnal (~1500 m) a lateral maximum of oxygen and lateral minima of nutrients are found at 25°-26°S at the crest of the Sala y Gomez Ridge. These property extrema imply an eastward flow at these latitudes.

Just below the Antarctic Intermediate Water, a marked low-oxygen tongue is seen to extend southward from 18°S to the southern end of the section. This middepth oxygen minimum and slightly shallower maxima of phosphate and nitrate are believed to be associated with the return flow of the deep and bottom waters that enter the North Pacific from the south [*Reid*, 1973a]. *Reid* [1986] has suggested that low-oxygen, high-nutrient water from the North Pacific crosses the equator at the eastern boundary and, after making an anticyclonic loop near 10°S, extends southward along the eastern boundary of the South Pacific. Our data indicate that along an isopycnal surface roughly coincident with the oxygen minimum, meridional minima of nitrate and phosphate occur at the equator accompanied by meridional maxima at 15°S (Figure 16). The minima at the equator dissociate high-nutrient water north of the equator from that along the eastern boundary of the South Pacific. It is not clear whether the North Pacific water crosses the equator at the eastern boundary or takes a more complicated path to the South Pacific.

A silica maximum is observed at 2500-3000 m in three locations: from the Southeast Pacific Basin to the southern Chile Basin, from 19°S to the Carnegie Ridge, and in the Guatemala Basin. It occurs at 36.96-36.99 σ_2 and appears to represent the southeastern edge of the ocean-wide deep silica maximum originated in the North Pacific.

The Southeast Pacific Basin deep water at 2800-3800 m contains a salinity maximum and a silica minimum. The former is roughly coincident with phosphate and nitrate minima, and the latter is about 500 m shallower than the salinity maximum. These extrema are a clear signature of the North Atlantic deep water. The salinity maximum deepens toward the north and intersects the bottom at 47°S on the southern flank of the Chile Rise, but the silica minimum extends into the southern Chile Basin.

The bottom water of the Southeast Pacific Basin is directly from the Lower Circumpolar Water flowing eastward in the Antarctic Circumpolar Current. It is colder, denser, fresher, and higher in oxygen and silica than the overlying deep water originated in the North Atlantic and is separated from it by a strong gradient of temperature centered at about 1°C. Blocked on the north by the Chile Rise, the bottom water of the Southeast Pacific Basin does not flow into the Chile Basin. The source of the bottom water in the Chile Basin appears to be shallower water at 3200-3400 m above the crest of the Chile Rise. The bottom water in the southern half of the Peru Basin may be supplied from the Chile Basin through the narrow passage (4900 m) along the Peru-Chile Trench at the northeast end of the Nazca Ridge and possibly also through the broad sill (3900 m) between the Nazca and Sala y Gomez ridges just east of our section. The bottom water in the northern half is lower in oxygen and higher in nutrients and appears to take a more devious route from these sills.

The bottom water we find in the Panama Basin can be supplied from the south through a saddle (at 86°W)

of the Carnegie Ridge, but its silica values are too high to be explained by this source. The bottom water in the Guatemala Basin is colder, more saline, denser, and higher in oxygen than Panama Basin waters at any depth, indicating that no inflow takes place from the Panama Basin to the Guatemala Basin to supply its bottom water. The Guatemala Basin bottom water must have come from the west across the East Pacific Rise as suggested by *Mantyla* [1975].

Acknowledgments. This study was supported by the National Science Foundation through grant OCE90-04394 as a component of the WOCE Hydrographic Program. The highly successful fieldwork is due to the dedicated support provided by the Oceanographic Data Facility at Scripps Institution of Oceanography and the captain and crew of R/V *Knorr*.

References

Bennett, E. B., An oceanographic atlas of the eastern tropical Pacific Ocean, based on data from EASTROPIC Expedition, October-December 1955, *Bull. Inter-Am. Trop. Tuna Comm., 8,* 33-165, 1963.

Brandhorst, W., Nitrification and denitrification in the eastern tropical North Pacific, *J. Cons. Int. Explor. Mer, 25,* 3-20, 1959.

Craig, H., W. S. Broecker, and D. Spencer, *GEOSECS Pacific Expedition,* vol. 4, *Sections and Profiles*, 251 pp., Nat. Sci. Found., Washington, D. C., 1981.

Cromwell, T., Thermocline topography, horizontal currents and "ridging" in the eastern tropical Pacific, *Bull. Inter-Am. Trop. Tuna Comm., 3,* 133-164, 1958.

Deacon, G. E. R., Comments on a counterclockwise circulation in the Pacific subantarctic sector of the Southern Ocean suggested by McGinnis, *Deep Sea Res., 24,* 927-930, 1977.

Deacon, G. E. R., Physical and biological zonation in the Southern Ocean, *Deep Sea Res., Part A, 29,* 1-15, 1982.

de Szoeke, R. A., On the wind-driven circulation of the South Pacific Ocean, *J. Phys. Oceanogr., 17,* 613-630, 1987.

Edmond, J. M., S. S. Jacobs, A. L. Gordon, A. W. Mantyla, and R. F. Weiss, Water column anomalies in dissolved silica over opaline pelagic sediments and the origin of the deep silica maximum, *J. Geophys. Res., 84,* 7809-7826, 1979.

Fine, R. A., and K. A. Maillet, Maintenance of the oxygen minimum zone in the eastern tropical Pacific, paper presented at the Pacific Basin Meeting, The Oceanography Society, Honolulu, July 19 to 22, 1994.

Hautala, S. L., and D. H. Roemmich, Subtropical mode water in the Northeast Pacific Basin, *J. Geophys. Res.,* in press., 1998.

Knauss, J. A., Equatorial current systems, in *The Sea: Ideas and Observations on Progress in the Study of the Seas,* vol. 2, *The Composition of Sea Water: Comparative and Descriptive Oceanography,* edited by M. N. Hill, pp. 235-252, Wiley-Interscience, New York, 1963.

Laird, N. P., Panama Basin deep water - Properties and circulation, *J. Mar. Res., 29,* 226-234, 1971.

Levitus, S., Climatological atlas of the world ocean, *NOAA Prof. Pap. 13,* 173 pp., U.S. Govt. Print. Off., Washington, D.C., 1982.

Levitus, S., and T. Boyer, World Ocean Atlas 1994, Vol. 4: Temperature, *NOAA Atlas NESDIS 4,* U.S. Department of Commerce, NOAA, NESDIS, Washington, D.C., 1994.

Levitus, S., R. Burgett, and T. Boyer, World Ocean Atlas 1994, Vol. 3: Salinity, *NOAA Atlas NESDIS 3,* U.S. Department of Commerce, NOAA, NESDIS, Washington, D.C., 1994.

Lonsdale, P., Abyssal circulation of the southeastern Pacific and some geological implications, *J. Geophys. Res., 81,* 1163-1176, 1976.

Lonsdale, P. F., and Malfait, Abyssal dunes of foraminiferal sand on the Carnegie Ridge, *Geol. Soc. Am. Bull., 85,* 1697-1712, 1974.

Love, C. M. (Ed.), *Eastropac Atlas,* vol. 1, Nat. Mar. Fish. Serv., Washington, D. C., 1972.

Lukas, R., The termination of the Equatorial Undercurrent in the eastern Pacific, *Prog. Oceanogr., 16,* 63-90, 1986.

Luyten, J. R., J. Pedlosky, and H. Stommel, The ventilated thermocline, *J. Phys. Oceanogr., 13,* 292-309, 1983.

Mantyla, A. W., On the potential temperature in the abyssal Pacific Ocean, *J. Mar. Res., 33,* 341-354, 1975.

Mantyla, A. W., and J. L. Reid, Abyssal characteristics of the world ocean waters, *Deep Sea Res., Part A, 30,* 805-833, 1983.

McCartney, M. S., Subantarctic Mode Water, in *A Voyage of Discovery, George Deacon 70th Anniversary Volume,* edited by M. Angel, pp. 103-119, Pergamon, Elmsford, N.Y. 1977.

McCartney, M. S., The subtropical recirculation of Mode Waters, *J. Mar. Res., 40,* suppl., 427-464, 1982.

McGinnis, R. F., Counterclockwise circulation in the Pacific subantarctic sector of the Southern Ocean, *Science, 186,* 736-738, 1974.

Neshyba, S., and T. R. Fonseca, Evidence for counterflow to the west wind drift off South America, *J. Geophys Res., 85,* 4888-4892, 1980.

Puls, C., Oberflächentemperaturen und Strömungsverhältnisse des Aequatorialgürtel des Stillen Ozeans, *Arch. Dtsch. Seewarte, 18* (1), 38 pp., 1895.

Reid, J. L., Jr., Intermediate waters of the Pacific Ocean, *Johns Hopkins Oceanogr. Stud., 2,* 85 pp., 1965.

Reid, J. L., Sea-surface temperature, salinity, and density of the Pacific Ocean in summer and in winter, *Deep Sea Res. Oceanogr. Abstr., 16,* suppl., 215-224, 1969.

Reid, J. L., Transpacific hydrographic sections at lats. 43°S and 28°S: The SCORPIO expedition, III, Upper water and a note on southward flow at mid-depth, *Deep Sea Res. Oceanogr. Abstr., 20,* 39-49, 1973a.

Reid, J. L., The shallow salinity minima of the Pacific Ocean, *Deep Sea Res. Oceanogr. Abstr., 20,* 51-68, 1973b.

Reid, J. L., On the mid-depth circulation of the world ocean, in *Evolution of Physical Oceanography: Scientific Surveys in Honor of Henry Stommel,* edited by B. A. Warren and C. Wunsch, pp. 70-111, MIT Press, Cambridge, Mass., 1981.

Reid, J. L., On the total geostrophic circulation of the South Pacific Ocean: Flow patterns, tracers and transports, *Prog. Oceanogr., 16,* 1-61, 1986.

Reid, J. L., On the total geostrophic circulation of the Pacific Ocean: Flow patterns, tracers and transports, *Prog. Oceanogr.,* in press, 1998.

Robinson, M. K., Atlas of North Pacific Ocean monthly mean temperatures and salinities of the surface layer, *Nav. Oceanogr. Off. Ref. Pub., 2,* 14 pp., 173 figs., Washington, D. C., 1976.

Roemmich, D., T. McCallister, and J. Swift, A transpacific hydrographic section along latitude 24°N: The distribu-

tion of properties in the subtropical gyre, *Deep Sea Res., Part A, 38,* suppl. 1, S1-S20, 1991.

Ruddick, B., A practical indicator of the stability of the water column to double-diffusive activity, *Deep Sea Res., Part A, 30,* 1105-1107, 1983.

Schott, G., Geographie des Indischen und Stillen Ozeans, 413 pp., Boysen, Hamburg, 1935.

Shulenberger, E., and J. L. Reid, The Pacific shallow oxygen maximum, deep chlorophyll maximum, and primary productivity, reconsidered, *Deep Sea Res., Part A, 28,* 901-919, 1981.

Stramma, L., R. G. Peterson, and M. Tomczak, The South Pacific Current, *J. Phys. Oceanogr., 25,* 77-91, 1995.

Stroup, E. D., The thermostad of the 13-C water in the equatorial Pacific Ocean, Ph D. dissertation, 205 pp., Johns Hopkins Univ., Baltimore, Md., 1969.

Sverdrup, H. U., M. W. Johnson, and R. H. Fleming, *The Oceans: Their Physics, Chemistry, and General Biology,* 1087 pp., Prentice-Hall, Englewood Cliffs, N.J., 1942.

Talley, L. D., Ventilation of the subtropical North Pacific: The shallow salinity minimum, *J. Phys. Oceanogr., 15,* 633-649, 1985.

Talley, L. D., Potential vorticity distribution in the North Pacific, *J. Phys. Oceanogr., 18,* 89-106,1988.

Talley, L. D., Distribution and formation of North Pacific Intermediate Water, *J. Phys. Oceanogr., 23,* 517-537, 1993.

Talley, L. D., Antarctic Intermediate Water in the South Atlantic, in *The South Atlantic: Present and Past Circulation,* edited by G. Wefer, et al., pp. 219-238, Springer-Verlag, N.Y., 1996a.

Talley, L. D., Tropical pycnostads and bottom boundary layers (abstract), *Eos Trans. AGU., 76(3),* Ocean Sci. Meet. Suppl., OS195, 1996b.

Talley, L. D., and T. M. Joyce, The double silica maximum in the North Pacific, *J. Geophys. Res., 97,* 5465-5480, 1992.

Talley, L. D., T. M. Joyce, and R. A. de Szoeke, Transpacific sections at 47°N and 152°W: Distribution of properties, *Deep Sea Res., Part A, 38,* suppl. 1, S63-S82, 1991.

Thomas, W. H., On denitrification in the northeastern tropical Pacific Ocean, *Deep Sea Res. Oceanogr. Abstr., 13,* 1109-1114, 1966.

Tsubota, H., Preliminary report of the Hakuho Maru cruise KH-71-5 (Phoenix Expedition), report, Ocean Res. Inst., Univ. of Tokyo, Tokyo, 1973.

Tsuchiya, M., Variation of the surface geostrophic flow in the eastern intertropical Pacific Ocean, *Fish. Bull., 72,* 1075-1086, 1974.

Tsuchiya, M., Subsurface countercurrents in the eastern equatorial Pacific Ocean, *J. Mar. Res., 33,* suppl., 145-175, 1975.

Tsuchiya, M., On the Pacific upper-water circulation, *J. Mar. Res., 40,* suppl., 777-799, 1982.

Tsuchiya, M., The subthermocline phosphate distribution and circulation in the far eastern equatorial Pacific Ocean, *Deep Sea Res. Part A, 32,* 299-313, 1985.

Tsuchiya, M., and L. D. Talley, Water-property distributions along an eastern Pacific hydrographic section at 135W, *J. Mar. Res., 54,* 541-564, 1996.

Warren, B. A., Transpacific hydrographic section at lats. 43°S and 28°S: The SCORPIO expedition, II, Deep water, *Deep Sea Res. Oceanogr. Abstr., 20,* 9-38, 1973.

Wijffels, S., J. M. Toole, H. L. Bryden, R. A. Fine, W. J. Jenkins, and J. L. Bullister, The water masses and circulation at 10°N in the Pacific, *Deep Sea Res., Part I, 43,* 501-544, 1996.

Wooster, W. S., Oceanographic observations in the Panama Bight, "Askoy" expedition, 1941, *Bull. Am. Mus. Nat. Hist., 118,* 113-151, 1959.

Wooster, W. S., Equatorial front between Peru and Galapagos, *Deep Sea Res. Oceanogr. Abstr., 16,* suppl., 407-419, 1969.

Wooster, W. S., and T. Cromwell, An oceanographic description of the eastern tropical Pacific, *Bull. Scripps Inst. Oceanogr., 7,* 169-282, 1958.

Wooster, W. S., and M. Gilmartin, The Peru-Chile Undercurrent, *J. Mar. Res., 19,* 97-122, 1961.

Wooster, W. S., T. J. Chow, and I. Barrett, Nitrite distribution in Peru Current waters, *J. Mar. Res., 23,* 210-221, 1965.

Wyrtki, K., Upwelling in the Costa Rica Dome, *Fish. Bull., 63,* 355-372, 1964a.

Wyrtki, K., The thermal structure of the eastern Pacific Ocean, *Dtsch. Hydrogr. Z.,* Erganzungsh. Reihe A, 84 pp., 1964b.

Wyrtki, K., Surface currents in the eastern tropical Pacific Ocean, *Bull. Inter-Am. Trop. Tuna Comm., 9,* 269-304, 1965.

Yuan, X., and L. D. Talley, Shallow salinity minima in the North Pacific, *J. Phys. Oceanogr., 22,* 1302-1316, 1992.

Mizuki Tsuchiya and Lynne D. Talley, Scripps Institution of Oceanography, University of California San Diego, La Jolla 92093-0230. (e-mail: ltalley@ucsd.edu)

(Received March 12, 1997; revised October 27, 1997; accepted November 21, 1997.)